Journal of Hydrology 597 (2021) 126170

Contents lists available at ScienceDirect

Journal of Hydrology

journal homepage: www.elsevier.com/locate/jhydrol

Research papers

Classification and trends in intermittent river flow regimes in Australia, northwestern Europe and USA: A global perspective

Eric Sauquet[a,*], Margaret Shanafield[b], John C. Hammond[c,1], Catherine Sefton[d], Catherine Leigh[e], Thibault Datry[a]

[a] INRAE, UR RiverLy, Centre de Lyon-Grenoble Auvergne-Rhône-Alpes, Villeurbanne, France
[b] Flinders University and National Centre for Groundwater Research and Training, Adelaide, Australia
[c] Department of Ecosystem Science and Sustainability, Colorado State University, Fort Collins, CO, USA
[d] UK Centre for Ecology & Hydrology, Wallingford, United Kingdom
[e] Biosciences and Food Technology Discipline, School of Science, RMIT University, Bundoora, Victoria 3083, Australia

ARTICLE INFO

This manuscript was handled by Andras Bardossy, Editor-in-Chief, with the assistance of Jie Chen, Associate Editor

Keywords:
Flow intermittence
Streamflow variability
River flow classification
Trend analysis

ABSTRACT

This study examines the spatial and temporal variability of flow intermittence over the period 1970–2018 across four countries (Australia, France, UK and the conterminous USA). Intermittence (no-flow periods) in 471 unregulated non-perennial rivers were analyzed using flow data collected from 1356 gauging stations distributed across the four countries. Climate data were also analyzed to place findings within a climate-change context. Intermittence of streamflow demonstrated high seasonality and showed regional differences. An aridity index was the most relevant explanatory factor of flow intermittence at the global scale; the more arid the climate, the higher the probability of non-perennial flow regimes. Flow intermittence was observed, however, in humid climate zones. A global classification of intermittent rivers was developed that included all the facets of the flow regime. This classification served as a basis for trend detection in annual frequency of no flows at the regional scale. Some, but not all, of the 14 examined regions in Australia and the US displayed significant trends and most of them displayed an upward trend in the occurrence of no-flow days.

1. Introduction

A large proportion of the channels comprising river networks globally cease flow or dry periodically (Larned et al., 2010; Datry et al., 2014; Leigh et al., 2016). These systems, collectively referred to here as intermittent rivers and ephemeral streams (IRES), range from near-perennial rivers with infrequent, short periods of no flow to rivers experiencing flow only following episodic rainfall (Snelder et al., 2013). The distribution of IRES is changing due to climate change, at the continental (Döll and Schmied, 2012), national (Sauquet et al., 2020a) and regional scales (Jaeger et al., 2014; Pumo et al., 2015; De Girolamo et al., 2017). Decreased minimum flows under climate-driven changes in the timing and magnitude of precipitation and runoff, and increases in temperature, could lead some perennial rivers to shift to non-perennial flow regimes and further reduce the flow permanence of some intermittent rivers. Conversely, many naturally intermittent rivers are becoming artificially perennial due to effluent recharge (e.g., Halaburka et al., 2013).

Globally, climate is a primary driver of streamflow patterns, though geology, topography and vegetation can also play dominant roles in space and time (e.g., Beaufort et al., 2019). Our global climate is not static, but subject to variability on many timescales. Trend analysis is one method of assessing how rivers respond to these changes in climate. The frequency of no flows, for example, is a key variable used to distinguish and classify IRES in large areas experiencing semi-arid to arid climate conditions (e.g., Kennard et al., 2010). However, flow intermittence is changing globally, and some areas of the globe are experiencing increasing frequency of flow intermittence as they become semi-arid, while warmer climate conditions can create flowing conditions in winter. Indeed the duration, timing and predictability of no-flow events along with their frequency are *all* important determinants of biodiversity and ecosystem processes, in both IRES and their adjacent or downstream ecosystems (e.g., Leigh and Datry, 2016). Detailed temporal descriptions of IRES hydrology, including the different facets of flow

* Corresponding author at: INRAE, UR RiverLy, Centre de Lyon-Grenoble Auvergne-Rhône-Alpes, Villeurbanne, France.
E-mail address: eric.sauquet@inrae.fr (E. Sauquet).
[1] United States Geological Survey MD-DE-DC Water Science Center, Baltimore, MD, USA .

https://doi.org/10.1016/j.jhydrol.2021.126170
Received 28 July 2020; Received in revised form 2 November 2020; Accepted 4 March 2021
Available online 9 March 2021
0022-1694/

intermittence, that follow a flow-regime classification methodology are thus necessary not only to summarize the hydrological behavior of rivers at various time scales but also to support environmental monitoring, water allocation decisions and environmental flow-setting (e.g., Kennard et al., 2010; Perez-Saez et al., 2017, D'Ambrosio et al., 2017).

To study flow patterns in rivers and how they change in time, we generally rely on gauging stations as the primary source of data. Although flow data from gauging stations only represents the overall hydrology at discrete locations (and indeed there is rarely more than one gauging station on a given intermittent river), gauging stations remain our chief source of time series data. For example, the frequency of no flows is a fundamental consideration when defining a river as non-perennial and thus is by far the most common metric used to characterize flow intermittence (e.g., Moliere *et al.*, 2009; Smakhtin and Toulouse, 1998; Bond *et al.*, 2010; Poff and Ward, 1989; Poff, 1996; Snelder et al., 2013; Eng et al., 2015). However, large scale comparison of gauging station data remains a challenge, due to limitations in the length of available time series, variability in the collection methods and reporting, and lack of information on the degree of catchment alteration due to anthropogenic activity in many regions of the world (e.g., Giuntoli et al., 2013; González-Ferreras and Barquín, 2017; Harrigan et al., 2018a; Yu et al., 2018). Yet, a large scale synthesis is essential; the scarcity of information on the occurrence of IRES, their flow regime patterns, and the environmental conditions that produce those patterns, are arguably the main reasons limiting their effective management (Snelder et al., 2013; Leigh et al., 2016). Characterizing the temporal hydrological patterns of IRES is an essential element of large-scale river management and research (Olden et al., 2011). Therefore, an overarching classification is needed to understand how IRES fit into a global continuum. This classification has begun, but to date has been regional or national. For example, Kennard et al. (2010) developed a classification of flow regimes for both perennial and non-perennial rivers in Australia, while a study specifically on non-perennial watersheds in the conterminous US primarily focused on seasonal occurrence of no flow in relation to climate, but did not quantify different elements of the no-flow regime using multiple metrics (Eng et al., 2015).

To address large-scale patterns and trends in IRES flow regimes, we explore long-term streamflow data from a large set of reference gauges across four countries spanning three continents. These data, combined with climate data, are then used in a:

i. Qualitative comparison of flow intermittence showing overarching commonalities and differences in flow characteristics.
ii. Examination of the importance of climate as a driver of flow regimes.
iii. Classification of IRES across all four countries using common metrics.
iv. Analysis of the trends in climate (specifically aridity and winter temperature) compared to trends in intermittence (in time and space) across the classifications.

This pan-continental study complements the expanding body of literature that has classified IRES in individual countries (Snelder et al., 2013; Kennard *et al.*, 2010; Buttle et al., 2012) and highlights commonalities and differences across IRES.

2. Methods

2.1. Selection of gauging stations

Daily discharge data were compiled using gauging station records from France, UK, Australia and the conterminous United States (US) (Table 1). These stations form subsets extracted from the nationwide reference hydrologic networks of the four countries. They were deeply screened and extensively used in global studies (e.g. Zhang et al. (2016) for Australia; Giuntoli et al. (2013), Hodgkins et al. (2017), and Renard and Thyer (2019) for France; Harrigan et al. (2018b), Gnann et al. (2019), and Smith et al. (2019) for the UK; Archfield et al. (2014), Hammond et al. (2018), and Dudley et al. (2020) for the US). The selection procedures are not strictly the same. However, the gauging stations were chosen to primarily reflect near-natural conditions. For example, only USGS gauging stations classified as "reference" by Falcone (2011) were used according to the quantitative and qualitative criteria of Falcone et al. (2010), which included calculation of a GIS-based disturbance index, visual inspection of topographic maps and imagery and use of information available in technical reports on human activities. Data quality was one of the stages of development of these networks. For example, the final selection of the French gauging stations stemmed from an iterative scheme including dialogue between researchers and data providers on monitoring conditions and possible non-natural causes of change (e.g. rating curve change, constructions affecting the river, change of the station location, etc.). In the UK, data quality was ensured by using gauging stations of the UK Benchmark Network (UKBN2) classed suitable for the study of trends in low flows, as by Barker et al. (2019) in their assessment of historical droughts. For more details on the selection procedures, see the references in Table 1. Three main criteria were imposed to select gauging stations that had: (i) a minimum length of 30 years of data between 01/01/1970 and 31/12/2018 with <5% of missing data, which resulted in the selection of gauging stations with at least 28.5 years of records, not necessarily continuous; (ii) no significant human influence on low flows; and (iii) high quality measurements in discharge (especially in low flows). A 30-year record length (with up to 5% missing data; criterion (i)) was considered the minimum to derive reliable statistics on hydrological extremes, such as those related to severe low and no-flows. This matches the timespan conventionally adopted to derive reliable statistics for climate (World Meteorological Organization convention WMO, 1989). To satisfy criterion (ii), gauging stations monitoring discharge of rivers with natural flows or minor abstractions were selected from previously published datasets (Table 1). A total of 1356 gauging stations across the four countries met all three criteria for inclusion in the final dataset.

Table 1
Main characteristics of the hydrological datasets compiled for this study – the interquartile ranges are given by values in brackets.

Country	Dataprovider & source	Number of gauging stations			Density (/1000 km^2)	Drainage area (km^2)	Record length (year)	Reference
		IR	WIR	PR				
Australia	Bureau of Meteorology http://www.bom.gov.au/water/hrs	131	32	59	0.03	338 [124; 662]	44.9 [41.9; 45]	Zhang et al. (2016)
France	HYDRO http://hydro.eaufrance.fr	12	29	161	0.37	95 [45; 175]	48.6 [45.8; 49]	Giuntoli et al. (2013)
UK	UK Benchmark Network https://nrfa.ceh.ac.uk/benchmark-network	3	4	94	0.42	25.7 [15; 27]	46.3 [44.9; 47.5]	Harrigan et al. (2018a)
Conterminous US	USGS http://waterdata.usgs.gov	162	98	571	0.10	309 [117; 775]	49 [43.4; 49]	Falcone (2011)

2.2. Characterising flow regimes for intermittent rivers

Hydrologically, distinguishing perennial from intermittent rivers is not straightforward and, perhaps in consequence, several definitions can be found in the literature. For example, Poff (1996) and Eng et al. (2015) considered a river "intermittent" if the mean number of zero-flow days was >10 d/yr and 15 d/yr, respectively. Poff (1996) stressed that the definition was rather arbitrary. Furthermore, Reynolds et al. (2015) discriminated "perennial" from two classes of intermittent rivers, considering a river as "weakly intermittent" when the mean number of zero-flow d/yr was <20, and "strongly intermittent" when it was >20. Leigh and Datry (2016) introduced the term "moderately" IRES, as intermediate between weakly and strongly IRES, to describe the results of a k-means clustering on a combined European and Australian dataset (in which rivers within each cluster had a mean of 11, 0.4 and 92 zero-flow d/yr, respectively). Huxter and van Meerveld (2012) suggested distinguishing "almost-intermittent rivers", for which the minimum daily river flow is <5 l/s, from "intermittent rivers", for which zero-flow conditions are observed. National regulations also define intermittent rivers including criteria on the annual number of zero-flow days (see D'ambrosio et al., 2017, for Italy and Spain).

In this paper, we considered a gauged river "intermittent" (IR) when the mean number of no-flow days in its 1970–2018 record was ≥5 d/yr, a definition supported by previous research on flow regimes in the countries of interest. We considered rivers with on average <5 d/yr but a strictly positive frequency of no-flow days in their record as "weakly intermittent" (WIR). All other rivers were considered "perennial" (PR).

The no-flow days were defined as only those days for which the observed daily flow was <1 l/s. This accounted for potential false-positive detection of no flows associated with measurement resolution constraints and uncertainty in discharge observations (Zimmer et al., 2020).

Each gauging station was characterized in terms of its river flow regime using statistics derived from daily-flow time series. There is a wide range of hydrological metrics used to characterize river flow regimes (e.g., Smakhtin, 2001; Olden and Poff, 2003). A set of 19 hydrological metrics calculated from daily-flow time series (Table 2) was selected for (i) their relevance for describing IRES and (ii) their complementarity in describing the different components of river flow regimes — magnitude, duration, timing, frequency, and rate of change of flows — introduced by Richter et al. (1996). The computation of and coding used for these metrics is given in Appendix A.

2.3. Climate metrics

Climate metrics were chosen first for their potential links to flow intermittence and second for their relevance regarding the ability to interpret results within a climate-change context. To this end, metrics were selected based on their simplicity of calculation (*i.e.* variables which could be easily derived from the outputs of the general circulation models). The final set of climate metrics included for analysis was mean annual temperature *MAT*, total precipitation *MAP*, an aridity index *AI* and mean winter temperature *MWT*. *AI* is computed as follows:

$$AI = MAP/MAPET \quad (1)$$

where *MAPET* is the Mean Annual Potential Evapotranspiration, respectively (Middleton and Thomas, 1997; Cherlet et al., 2018), and the UNEP classification consider a location "hyper-arid" if $AI < 0.03$, "arid" if $0.03 < AI < 0.2$, "semi-arid" if $0.2 < AI < 0.5$, "dry sub-humid" if $0.5 < AI < 0.65$ and otherwise "humid" ($AI > 0.65$). In this application, *MAP* and *MAPET* are average values over the gauged basins.

Due to limited access to climate data for all the gauging stations examined and to the need for consistency, we used the gridded TerraClimate product (Abatzoglou et al., 2018), which is available at 4 km spatial resolution and 1 month temporal resolution back to 1950. Monthly time series of each variable were extracted as watershed-averaged means to watershed boundaries available from national gauging network repositories using the *exactextractr* R package (Baston, 2020). Where watershed boundaries were not available for a subset of the gauges, the gauging location was used in combination with MERIT hydrography (Yamazaki et al., 2019) to prepare watershed boundaries based on upstream contributing area. Monthly time series were then aggregated to annual and mean annual time series by calculating annual totals of precipitation and potential evapotranspiration and means of maximum, minimum, mean and winter mean temperature, where winter months for France, the UK and USA are December, January and February, and for Australia are June, July and August.

The identification of the main climate drivers was based on the analysis of homogeneity within classes derived from the empirical distribution of climate metrics. Classes were first defined by *N* quantiles for *N*-1 evenly spaced cumulative probabilities ($1/N$, $2/N$…, $(N-1)/N$) derived from the empirical distribution of each climate descriptor. The proportion of each type of river (%*IR* for IR, %*WIR* for WIR and %*PR* for PR) within each class was then computed. Secondly the proportions %*IR*, %*WIR* and %*PR* were computed for each class as well as the inter-class variance related to each partition. The three inter-class variances measure the degree of separation between classes and the highest value indicates the highest discrimination power among the tested partitions.

Four partitions of IRs were derived from each of the four empirical distributions of the selected climate metrics *MAT*, *MAP*, *AI* and *MWT*. The samples of climate metrics were divided into 10 bins defined by the minimum, the nine deciles and the maximum. Each class had the same size (135 or 136 gauged basins), which is a size large enough to derive robust statistics.

2.4. Classification procedure

We performed a simple classification based on a hierarchical agglomerative cluster analysis using Ward's minimum variance method

Table 2
Hydrological metrics selected to characterize river flow regime.

Aspect	Name	Definition
Intermittence	*F0*	No-flow probability defined by the number of days with no flow per year (day/yr)
Magnitude	*Qp*, $p = 1, 5, 90, 95$	Daily flow exceeded 1, 5, 90, 95% of the time derived from the flow duration curve (m3/s)
Duration	*meanD*, *medianD*, *sD*	Mean, median and standard deviation of the duration of no-flow events† (day)
	D80	Duration of the longest no-flow event during the year with an empirical return period of 5 years (*) (day)
Frequency	*meanN*, *medianN*, *sdN*	Mean, median and standard deviation of the number of no-flow events† per year (/yr)
Timing	θ, *r*	Mean timing of no-flow events† and the dispersion around, based on circular statistics (*) (dimensionless)
	Sd6	Seasonal predictability of dry periods (*) (dimensionless)
Rate of change	*Drec*	Seasonal recession time scale (Catalogne, 2012) (day)
	Ic	Concavity index derived from the flow duration curve, introduced by Sauquet and Catalogne (2011) (*) (dimensionless)
	BFI	Baseflow index computed with the smoothed minima method introduced by the Institute of Hydrology (1980) (dimensionless)
	medianDr	Median duration of runoff event (*) (day)

† A no-flow event is a period of consecutive no-flow days; * see Appendix A for calculation details

and the Euclidean distance between metrics as similarity criteria. Note that the coordinates of the gauging stations were not included in the distance between clusters and that methods leading to contiguous regions (e.g., Assunção et al., 2006; Guo, 2008) were not applied here; instead, our methods provide a purely hydrological characterization based on river flow regimes. The classification was achieved using a subset of weakly correlated climate metrics and hydrological metrics, from among those described above, as identified by a Principal Component Analysis (PCA) performed on all the metrics and regression analyses among pairs of metrics (Olden and Poff, 2003). The three first principal components explained 63% of the total variance in the dataset including the 19 hydrological metrics and the two main climate drivers *AI* and *MWT*. The first component had large positive loadings for *F*0 and for all flow metrics related to the duration. Metrics related to flow duration curve characteristics, aridity and predictability were highly negatively correlated with the first axis. The second principal component is positively correlated with all duration metrics and negatively correlated with frequency metrics. Metrics related to no-flow events were weakly correlated with the third axis. The final subset of hydrological metrics includes:

- Seven metrics (*F*0, *medianD*, *sdD*, *meanN*, *sdN*, θ, *r*), which focus specifically on no-flow conditions. The first metric *F*0, when expressed in terms of percentage of the time with no-flow conditions, can be interpreted as flow permanence and is an important determinant of river biodiversity. Statistics on the duration and number of no-flow events (*medianD*, *sdD*, *medianN*, *sdN*) provide information complementary to flow permanence on the dynamics of flow intermittence, *e.g.*, the way no-flow events are distributed within the year and their average severity in terms of consecutive days without flow. Circular statistics *r* and θ were also calculated to characterize periodicity of phenomena which contain temporal seasonal components. These metrics were initially developed to identify flood periods on the basis of the timing of annual maximal peak discharges (e.g., Burn, 1997; Castellarin et al., 2001) and have been applied to characterize low-flow periods when discharge falls below a critical threshold value (e.g., Prudhomme *et al.*, 2016). Here, *r* provides a measure of the regularity of no-flow days while θ gives the mean date of no-flow occurrence.
- Four metrics (*Qp*, $p = 1, 90$, *IC* and *medianDr*), derived from the flow duration curve, describing low to high flow components.
- Two metrics (*Drec* and *medianDr)*, which are durational measures of time recession at the seasonal scale and of flood dynamics, respectively.

The metrics related to no-flow conditions are overrepresented in the list of selected metrics, in accordance with the objective of characterizing flow regime of IRES. Further transformations were applied to normalize metrics and reduce asymmetry in empirical distributions: the metrics related to duration *medianDr, meanD, medianD, sdD* were log-transformed; *Qp*, $p = 1, 90$ were divided by the mean long-term annual discharge before being square-root transformed; *F*0, *medianN*, *sdN, Drec* and *Ic* were square-root transformed. The mean date θ was transformed to allow comparison of the timing with no-flow conditions accounting for the shift in seasons between the two hemispheres. The variables $r \times \sin(\theta)$ and $r \times \cos(\theta)$ were used instead of *r* and θ to avoid an artificial break in winter induced by angles.

2.5. Trend analysis

Trends were investigated at the aggregated level of clusters of gauged basins. To overcome some of the issues due to both spatial and temporal dependencies between sites, the analysis was conducted using regional metrics, following Ribes et al. (2019), here derived from the at-site annual *F*0. First, values were computed for each river and year and converted into non-exceedance probabilities. When annual *F*0 was available for more than eight IRs, the median of these annual values was then calculated for each homogeneous group of rivers, and this regional metric was used to represent flow intermittence at the regional scale. The regional metric was not available over the whole period 1970–2018 due to gaps in the discharge records. Trends in regional flow intermittence were evaluated using the non-parametric, modified Mann–Kendall trend test accounting for autocorrelation in time series (Yue and Wang, 2004), the Theil-Sen slope estimator (Theil, 1950; Sen, 1968) and least-squares linear regression for graphic representations. The Regional Kendall test (Helsel and Frans, 2006) was applied to identify evidence of consistent trend at multiple locations. The choice of the method is partly supported by results of Renard et al. (2008), showing on the basis of simulated fields that the method applied here is unbiased and well suited for regional stationarity analysis, and performs as well as - for example – the regional average Mann-Kendall test developed by Yue and Wang (2002). Positive (or negative) slopes suggest trends of more (or less) frequent years with no-flow conditions. Time-series demonstrate statistically significant trends when *p*-values obtained from the Mann-Kendall test were less than the predetermined significance level (0.05).

3. Results

3.1. Flow characteristics in IRs

A set of 471 stations (308 IRs and 163 WIRs) out of the 1356 met the criteria for intermittence (Table 1, Fig. 1). Record lengths of IRs ranged from 28.7 to 49 years, with continuous observations throughout the 1974–2014 period available for 80% of the stations. The extended overlapping period enabled comparisons between flow statistics. The drainage areas of IRs ranged from 4 to 232,850 km^2, with a dominant proportion of small to medium size catchments (50% have catchment areas of 110–650 km^2). >50% of IRs recorded no flow for at least 10% of their record length. Of the flow regime statistics, the median number of continuous periods with no-flow days (*medianN*) showed the most heterogeneous pattern within countries (particularly in the US; not shown).

There were also distinct regional differences in the occurrence of continuous periods with no-flow days. Within countries, the proportion of PRs was lowest in the UK and highest in Australia, where 73% of all stations recorded no-flow days (Table 1). Across all countries, nearly 90% of the 471 IRs and WIRs were located in Australia and the conterminous US. The proportion of IRs among the gauged rivers was distributed relatively evenly over Australia except for the interior and central west, where no perennial gauges were identified and values of *F*0 are markedly higher (Fig. 1). Most of the gauged basins with low values of *F*0 were located along the southern and eastern coast while high values were in central (arid and semi-arid) Australia. In France, most IRs were located in the west and the south-western coastal region, and *F*0 was low throughout the country (50% of the IRs demonstrate *F0* above 9 d/yr). In the UK, only three IRs and four WIRs were identified. However, one station demonstrated a high value of *F*0 (173 d/yr) while the two others had values of *F0* below 15 d/yr. In the US, the interquartile range of *F*0 was 17–124 d/yr, with the majority of IRs located on the West coast and in the central states (*i.e.* in the Great Plains). Most of the high values of *F*0 were concentrated in the central part of the country. Flow intermittence was infrequently recorded in mountainous regions and absent from eastern mountain gauges.

Flow intermittence was highly seasonal, but seasonality also varied substantially from one country to another (Fig. 2). Most of the gauged IRs (58% for Australia, all for France and UK, 72% for the USA) experienced, on average, no flow in summer and early autumn (between June and September in the Northern Hemisphere and between December and March in the Southern Hemisphere). In Australia and the US, gauged basins with θ (mean date of no-flow occurrence) falling outside of summer periods tended to demonstrate low seasonality: the median of *r* for these basins (0.36 for Australia, 0.32 for the US) was lower than for basins with no-flow periods on average in summer (0.58

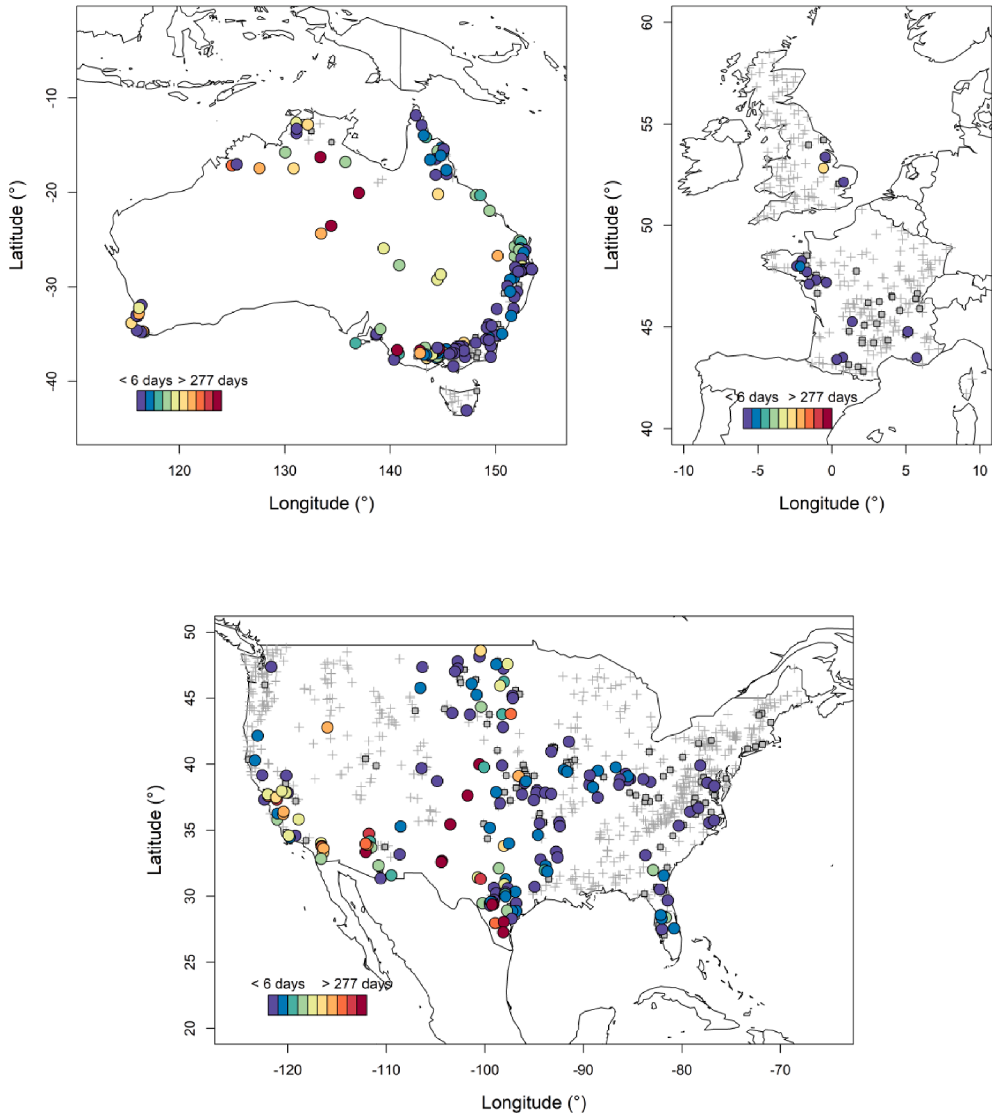

Fig. 1. Mean total number *F*0 of no-flow days per year (O intermittent river; ☐ weakly intermittent river; + perennial river).

for Australia, 0.66 for the US).

3.2. Climate as a driver of flow intermittence

The partition based on *AI* resulted in the maximal inter-variance of %*IR*, %*WIR* and %*PR*. The metric *AI* was globally the most suitable variable for discriminating IRs from PRs. The climate metrics ranked second and third in terms of power of discrimination were the mean annual temperature *MAT* and the total precipitation *MAP*, respectively. From the four climate metrics, only *AI* and *MWT* are considered in the following analyses. The metric *MWT*, despite weak overall discriminating power, was finally selected because it was the only climate metric that could distinguish between no-flow conditions due to freezing versus no flow from other causes. Note that *AI* was square-root transformed before using this climate metric in the clustering procedure to reduce asymmetry of the empirical distribution.

Overall, %*IR* was higher when *AI* was lower (*i.e.* when climate was more arid) and %*IR* was lower when *AI* was higher (*i.e.* when climate was more humid) (Fig. 3d). This global tendency was shared across the countries. However, the distribution of IRs differed among and within countries, in particular with the pattern for Australia contrasting from other countries (Fig. 3a). The contrasting results among countries in terms of discriminating IRs from PRs were due to non-overlapping ranges in *AI* and the specificity in climate conditions (e.g., the proportion of gauged basins with negative winter temperatures was the highest in the US (Fig. 3c); the proportions of semi-arid basins and dry sub-humid basins were comparable but were not found in France or the UK (Fig. 3b).

Finally, the link between levels of intermittence and aridity (Fig. 4) was summarized using the UNEP classification. We computed %*IR*, %*WIR* and %*PR* for each climate type as defined by the aridity index, *AI* (Table 3). Only nine gauged basins (two in the US and seven in Australia) experienced “arid” conditions, so they were pooled with “semi-arid” basins, leading to the “arid & semi-arid” class. Proportions were interpreted in terms of probability. Under arid, semi-arid and dry sub-humid conditions, the probability of a river basin being non-perennial was around 63% when $AI < 0.65$. This probability declined to around 14% under humid conditions.

3.3. Classification of intermittence

The classification procedure was applied to the 308 IRs using the subset of 14 climate and hydrological metrics (Figs. 5 and 6, Appendix B). A specific color was attributed to each class in Figs. 5 and 6 and the color palette was used latter to distinguish the different classes in subsequent graphs. According to the agglomeration schedule, the

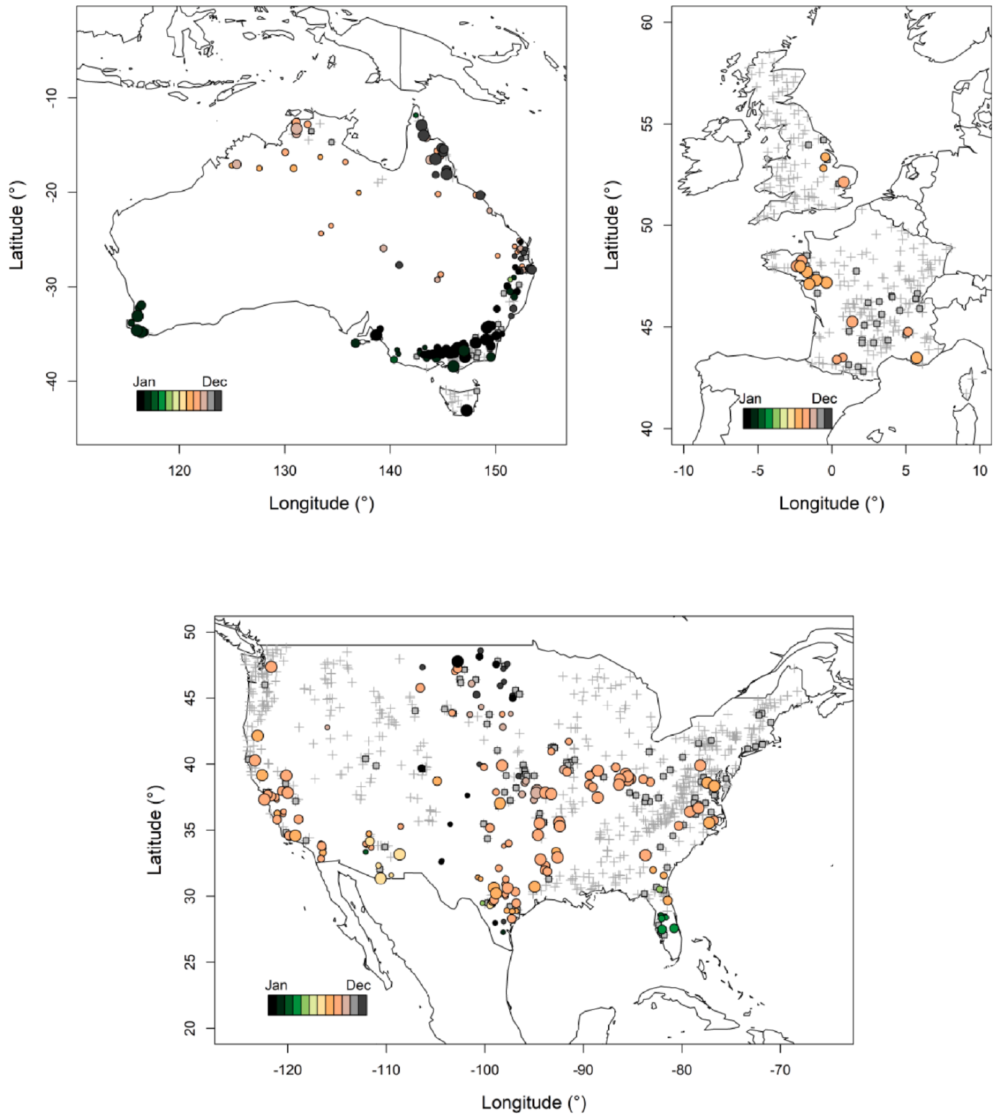

Fig. 2. Mean timing θ and dispersion r around θ (O intermittent river; □ weakly intermittent river; + perennial river) – the size of the dot is inversely proportional to r.

hierarchical cluster analysis suggested solutions with two, six and nine groups. The solution with two groups mainly differentiated IRs according to their degree of flow intermittence (the interquartile ranges of $F0$ of the two groups did not overlap). At least six groups were required to distinguish 15 IRs experiencing continental climate with cold winters and hot summers in the US as a separate group. The solution with nine groups identified six harsh IRs that had very few days with flow conditions. Moreover, this solution resulted in a near uniform number of gauged basins obtained per group (six classes with 40–52 basins, and three classes with 6–24 basins). Hydrographs observed at one gauging station illustrated the seasonal pattern of river flows within each group (Fig. 7). The distribution of the nine groups across the four countries is detailed in Table 4 and in Fig. 8.

The classification discriminated against rivers primarily on the basis of the mean annual proportion of no-flow days (Fig. 5). IR Groups 1–5 were classified as weakly to moderately intermittent. There was a non-negligible probability for these groups to experience a full year with no-flow conditions (see the distribution of *medianN*). Groups 6–9 contained 126 moderately to harshly, regularly intermittent rivers (with $F0 > 10\%$ for all but five gauged basins of Group 6).

Although most of the basins (1110 with $AI > 0.65$ among the 1356 gauging stations) experienced humid climates, a wide diversity of seasonal patterns was identified in the classes of IRs (Fig. 7), ranging from rainfall-fed regimes with high flows in winter and low flows in summer (Groups 1, 2 and 3) to snowmelt-dominated regimes with high flows in spring or early summer and winter minima caused by freezing (Groups 3 and 5). Groups 1, 2, 3 and 8 displayed intermittence in summer and early fall while Groups 4, 5 and 7 experienced intermittence in spring and winter (Fig. 6). Seasonality of no-flow conditions was not pronounced for Groups 6 ($r \sim 0.25$) and 9 ($r \sim 0.001$). Group 7 and Group 8 were comparable in terms of frequency of flow <1 l/s but differed in the distribution of no-flow events each year. Group 1 was the most frequently observed in our dataset, and the most relevant for European rivers. Group 7 was specific to Australia while Groups 3 and 5 were primarily associated with Midwest US (with few exceptions).

Direct use of the nine groups defined above to study stationarity in flow intermittence was not straightforward because the groups encompassed a wide variety of climates, and this was particularly evident in Australia and the US. Therefore, sub-groups were delineated at national or regional levels (Fig. 8). Related regions were outlined manually to ensure geographic consistency (median size = 11° lat × 20° long, since climate; the regions have been created considering a smaller extension in latitude than in longitude since latitude is a more important factor influencing climate patterns than longitude at the global scale) and to

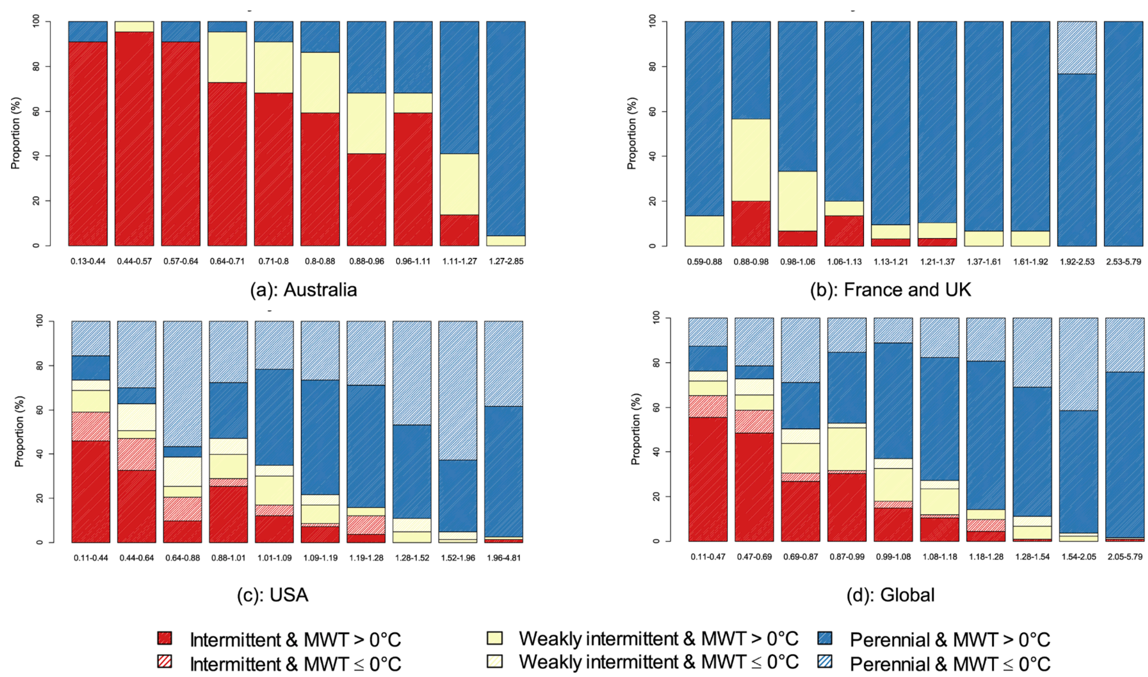

Fig. 3. Proportion of intermittent rivers (*%IR*), of weakly intermittent rivers (*%WIR*) and of perennial rivers (*%PR*) by class of *AI* (the limits of the classes are defined by the deciles of the *AI* values).

limit heterogeneity in climate conditions, considering the Köppen-Geiger climate classification (Peel et al., 2007).

Basins of Group 1 in Europe that were located in southern France (with latitude $< 46°$) were extracted to form one sub-group under oceanic influence. East-west distinctions were considered for the US to delineate the two regions 8 W ($-124 < \text{long} < -106$ and $30 < \text{lat} < 39$) and 8E ($-105 < \text{long} < -81$ and $28 < \text{lat} < 41$). Finally, stationarity within 14 regional pools (7 in the US, 1 crossing France and UK, and 6 in Australia) with >8 gauged basins in each pool were analyzed.

3.4. Trend analysis

High year-to-year variability of flow intermittence was observed (Figs. 9–11), with specific climatic events standing out in the data as high values of median non-exceedance probability with small whiskers. In Australia, the data were anomalous in Groups 1 and 2 (Fig. 9) in 1982–1983, and from 2000 to 2009 all Groups but Group 7 had a high proportion of no-flow conditions. Likewise, in Europe there were notable periods of high no-flow frequency in 1976 and from 1989 to 1992 in Group 1 (Fig. 10). In the eastern US, the year 2012 was marked by extremely dry conditions. Due to the particular cause for intermittence (freezing), the temporal pattern displayed for Group 5 differed substantially from those for other Groups (Fig. 11).

Despite the strong variability observed in the time series, statistically significant trends (*i.e. p-value* < 0.05) were detected when applying the Modified-Mann Kendall test for eight of the 14 groups. All but one significant trend was positive, indicating an increase in flow intermittence. The slight trend of increasing flow intermittence in Europe was not significant. Coherent results were found for groups with overlapping regions in southern Australia (1, 2, 6 and 8). Regardless of differences in significance level, the slopes in southern Australia were all positive. Upward trends were found in south central states of the US (2 and 6). However, these upward trends were not statistically significant due to serial autocorrelation in regions 8 W and 8 E. Region 5 in the US displayed a decrease in flow intermittence.

Out of the 14 regions examined in Table 5, eight exhibited a statistically significant temporal change though no change was found in Europe. A question relates to the consistency of the detected changes in flow intermittence with changes observed in the main climate drivers *AI* and *MWT* (Section 3.2) over the same period at the regional scale. For each region, we carried out the regional Mann Kendall trend test to test for trends in *AI* and *MWT* in the gauged basins distributed across the regions. Significant changes in *AI* were observed for 5 out the 14 regions (Table 5). Here, the consistency in the sign of the changes was expected rather than consistency in the level of significance (the sensitivity of flow intermittence to changes in climate drivers varied between catchments) and, in the case of consistency, it does not mean that causal links are established. In Australia, the five regions with detected increase in flow intermittence experienced increase in *AI*. Conversely, no changes in both *AI* and flow intermittence were detected in Europe. The consistency was less noticeable in the US. However the sign of the change in *AI*, although not significant, was consistent with the changes in flow intermittence. Note that for region 5, where *AI* was influenced by freezing, no significant change was detected in the winter temperature *MWT*. The slight trend towards warmer winter combined with more precipitation (not shown here) may be sufficient to result in decreased in flow intermittence.

4. Discussion

4.1. Spatial pattern of flow intermittence

The proportion of IRES in the database is substantial: 25% and 15% of the gauging stations are intermittent (IR) and weakly intermittent (WIR), respectively. However, the gauged IRs are not uniformly distributed. >50% of the IRs in the database are located in Australia, where only 35% of the stations are considered perennial. In the UK, the proportion of IRs and WIRs in the near-natural network is low (5% of the 146 UKBN2 gauging stations). Rivers with gauged intermittent regimes but without human influence are rare; intermittence in the wider UK hydrological monitoring network is more prevalent (Tramblay et al., 2020). Two of the three IRs are small, clay headwater catchments (<30 km^2), whilst chalk catchments in the south east of England are notably absent because of the historical effects of abstraction (Westwood et al., 2017). Furthermore, it is likely that intermittence in the UK, and more widely in temperate zones, is under-represented in the hydrological

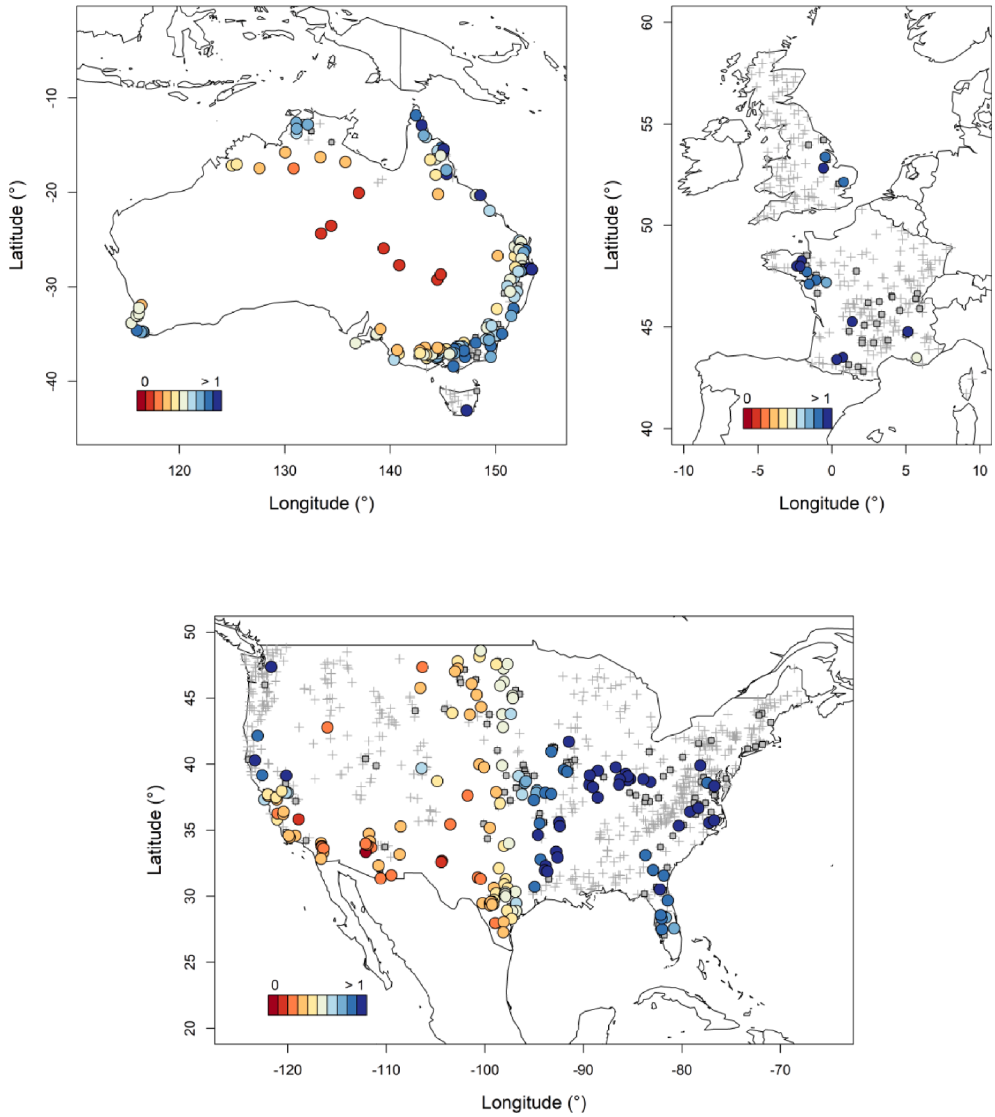

Fig. 4. Aridity index (● intermittent river; □ weakly intermittent river; + perennial river).

Table 3
Proportion of intermittent rivers (*%IR*), weakly intermittent rivers (*%WIR*) and of perennial rivers (*%PR*) by class of aridity.

Country	Number of gauging stations	% of intermittent rivers (%IR)	% of weakly intermittent rivers (%WIR)	% of perennial rivers (%PR)	Climate
Australia	34	91%	3%	6%	arid & semi-arid
	35	91%	3%	6%	dry sub-humid
	153	44%	20%	36%	humid
France and UK	3	33%	0%	67%	dry sub-humid
	300	5%	11%	84%	humid
Conterminous USA	117	56%	15%	29%	arid & semi-arid
	57	46%	16%	39%	dry sub-humid
	657	11%	11%	78%	humid
All	151	64%	12%	24%	arid & semi-arid
	95	62%	11%	27%	dry sub-humid
	1110	14%	12%	74%	humid

monitoring network (Stubbington et al., 2017); certainly in France, most IRs remain ungauged. The spatial pattern of IRs across France is consistent with Beaufort et al. (2018), who show gauging stations and sites from the ONDE network with observed no-flow conditions between 2012 and 2017. Although WIRs are found across France, there are clusters of gauging stations in the western and southwestern regions. Note that there are more WIRs in France than IRs, which provides an opportunity to study shifts from rarely towards moderately intermittent streams. This is also true in the US where nearly 20% of the selected gauging stations is on intermittent rivers (Table 1). This suspected underestimation is consistent with conclusions from previous national studies: IRs may represent around 60% of total river length in the conterminous US (Nadeau and Rains, 2007). The distribution of IRs across the US is similar to the results of Eng et al. (2015), for which

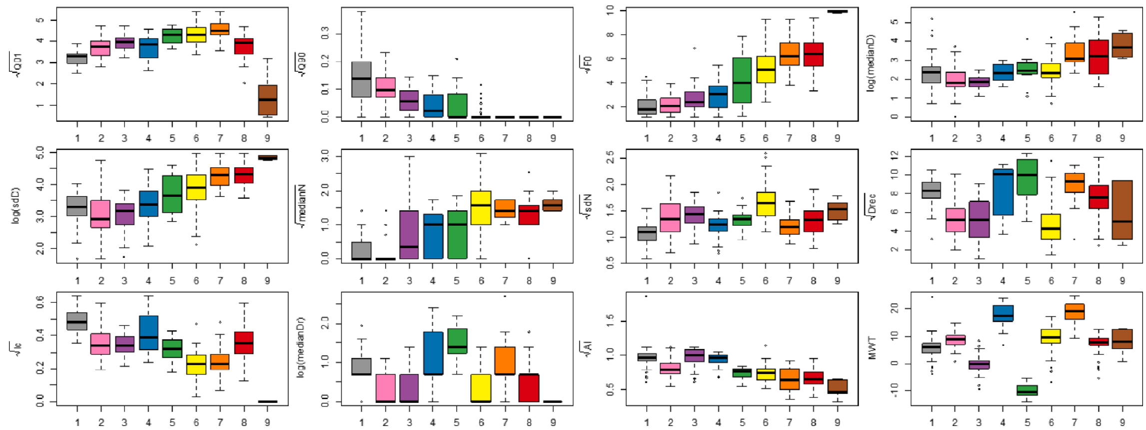

Fig. 5. Box plots of the variables used in the clustering procedure for each class. The boxplots are defined by the first quartile, the median and the third quartile. The whiskers extend to 1.5 of the interquartile range; open circles indicate outliers. A specific color is attributed to each group and the number of the Group is given along the x-axis.

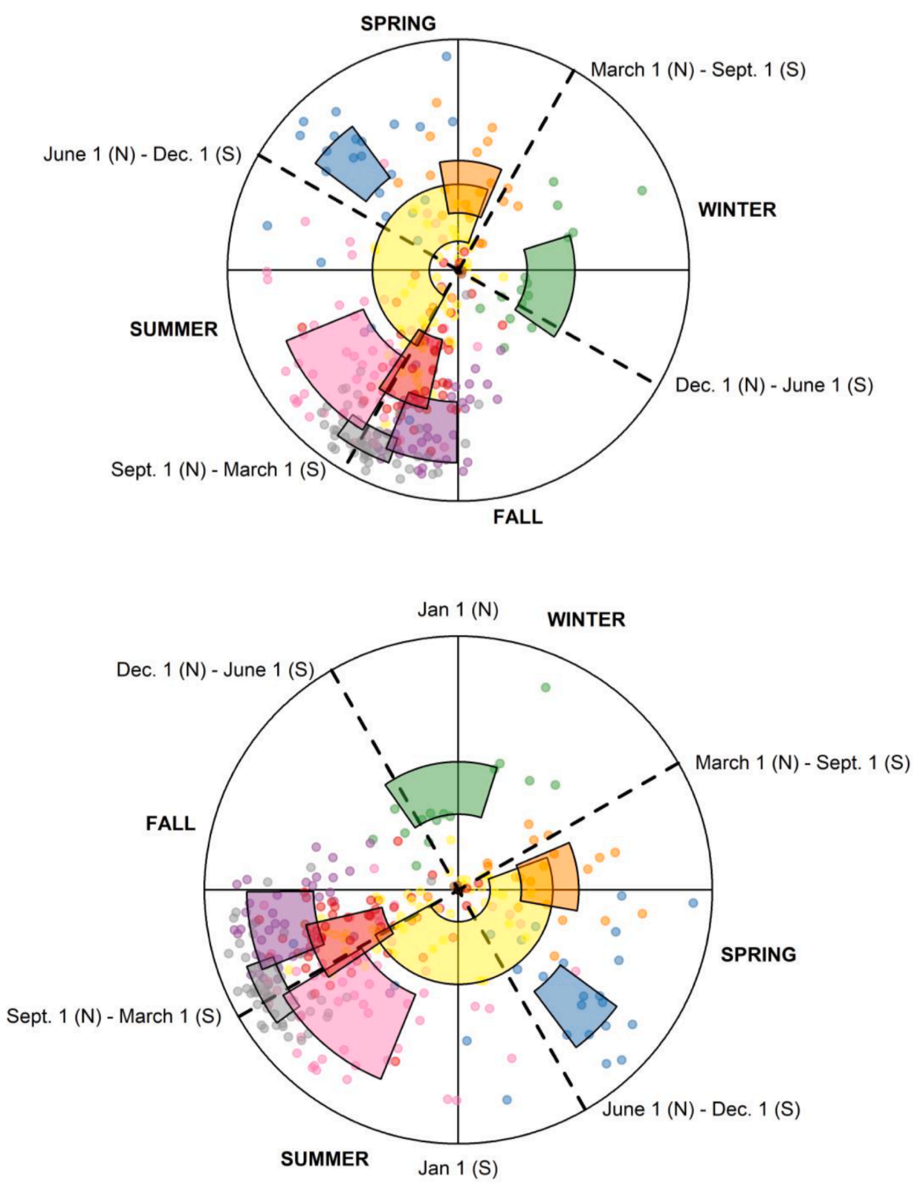

Fig. 6. Distribution of the circular variables for each class. This representation was adopted to display the distribution of the directional statistics r and θ and to facilitate interpretation of seasonality: (i) the areas are defined by the first quartile and the third quartile of r and θ, and (ii) each dot is related to one river and the color is associated with the membership to one group. Note that the dashed lines indicate the start of four meteorological seasons (S: South Hemisphere; N: North Hemisphere).

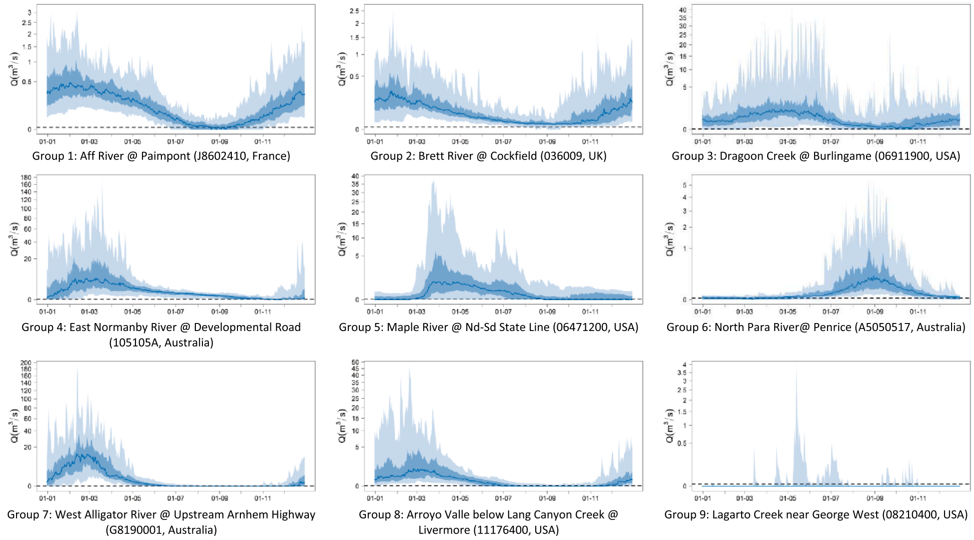

Fig. 7. Median annual hydrographs for nine examples of each Group of IRs. Shaded areas indicate the 90% and interquartile ranges, median hydrograph is in dark blue and the y-axis displays a square-root scale. Dashed lines identified the 1 l/s threshold used to define no-flow conditions. (For interpretation of the references to color in this figure legend, the reader is referred to the web version of this article.)

Table 4
Number of basins per group and per country.

Country	Group								
	1	2	3	4	5	6	7	8	9
Australia	21	27	0	15	0	33	20	15	0
France	9	1	1	0	0	1	0	0	0
UK	1	1	1	0	0	0	0	0	0
Conterminous US	20	23	38	9	15	16	0	35	6
All	51	52	40	24	15	50	20	50	6

gauging stations were also extracted from the GAGES2 database. However, other constraints were applied: a threshold of 15 d/yr was imposed to distinguish perennial from intermittent rivers and the required length of records between 1950 and 2012 was set at 10 years. Finally, stations located in the US that have shoreline on the east coast and in northwestern US are absent from the dataset examined by Eng et al. (2015). While these estimates are limited in spatial extent, they suggest that the IRES are extremely abundant globally.

4.2. Drivers of flow intermittence

Aridity (as measured by *AI*) was the most relevant climate driver within the set of selected metrics. *AI* is a measure of dryness based on precipitation and evapotranspiration processes related to air temperature, which may explain why it outperformed the individual precipitation (*MAP*) and temperature (*MAT*) variables. The list of potential climate drivers examined in this study was intentionally limited. Indeed, the potential climate drivers were primarily selected for the availability from GCM outputs and the reliability of the projected change under global warming conditions. Indicators related to climate extremes were thus not considered here. Aridity is certainly not the single main driver of intermittence: rivers may cease flowing under humid conditions (12% of the gauging stations with $AI > 1.41$). For example, many streams in Australia's wet-dry tropics are intermittent (Leigh and Sheldon, 2008). Furthermore, Warfe et al. (2011) suggest that, in addition to climate, latitude and geology control flow intermittence at a regional scale in Australia. A geological origin of flow intermittence is likely in both France and the UK, and globally at the European scale (Sauquet et al., 2020b); no-flow conditions are mainly due to impervious bedrock in western France (crystalline rock formation), to groundwater-table fluctuations and seepage through permeable channels in northern and southwestern France (sedimentary rock formation), and to the presence of an extensive karst in eastern France (Jeannin et al., 2016). In southern France, Mediterranean climate conditions may have a moderate influence on flow intermittence (Couturier and Fourneaux, 1998). In the UK, flow intermittence driven by permeable geology is observed in soluble rocks; for example in the Carboniferous Limestone of the Peak District (Stubbington et al., 2009), and in the Cretaceous Chalk of south and east of England, where streams typically contract through the summer months (Sefton *et al.*, 2019). Many of the intermittent watersheds in humid portions of the US contain significant karst developments which may explain flow intermittence. For example, a large part of Florida is karstic with high hydraulic conductivity so that by the end of the dry season (*i.e.* January- June) many streams become intermittent.

4.3. Classification and dynamics of intermittent rivers

Many river flow classifications based on a set of gauging stations do exist, including those encompassing a small to large portion of IRs (e.g. Kennard et al., 2010; Oueslati et al., 2015) as well as those restricted to IRs (e.g., Eng et al., 2015). There are many ways to establish a classification in accordance with predefined objectives (see Olden et al., 2011) and as a consequence the "universality" of any one classification is debatable. A large set of hydrological indices related to the different components of river flow regimes were considered in this study. In accordance with the objective of developing a classification dedicated to IRs, the metrics related to no-flow periods were overrepresented to give more weight to flow intermittence in the production of homogenous groups of rivers. Links between our results and previous classifications can be identified. For example, Eng et al. (2015) emphasized the seasonality of no-flow periods, which is one component of flow intermittence amongst others considered here in our clustering procedure. Most of the "fall-to-winter" IRs in west-north-central US of Eng et al. (2015) are classified within our Group 5 rivers, with IRs experiencing negative winter temperatures and no-flow events in autumn or winter (Fig. 11). "Non-seasonal" IRs are found in Groups 7–9, which displays the least seasonally contrasted temporal pattern of no-flow periods ($r \sim 0.35$, Fig. 6). The linkage with the Australian river flow classes developed by Kennard et al. (2010) is not straightforward due to the presence of perennial rivers in that dataset. Classes 5–8 of Kennard et al. (2010), which include IRs from Groups 1, 2, 6 and 8 of our classification, are

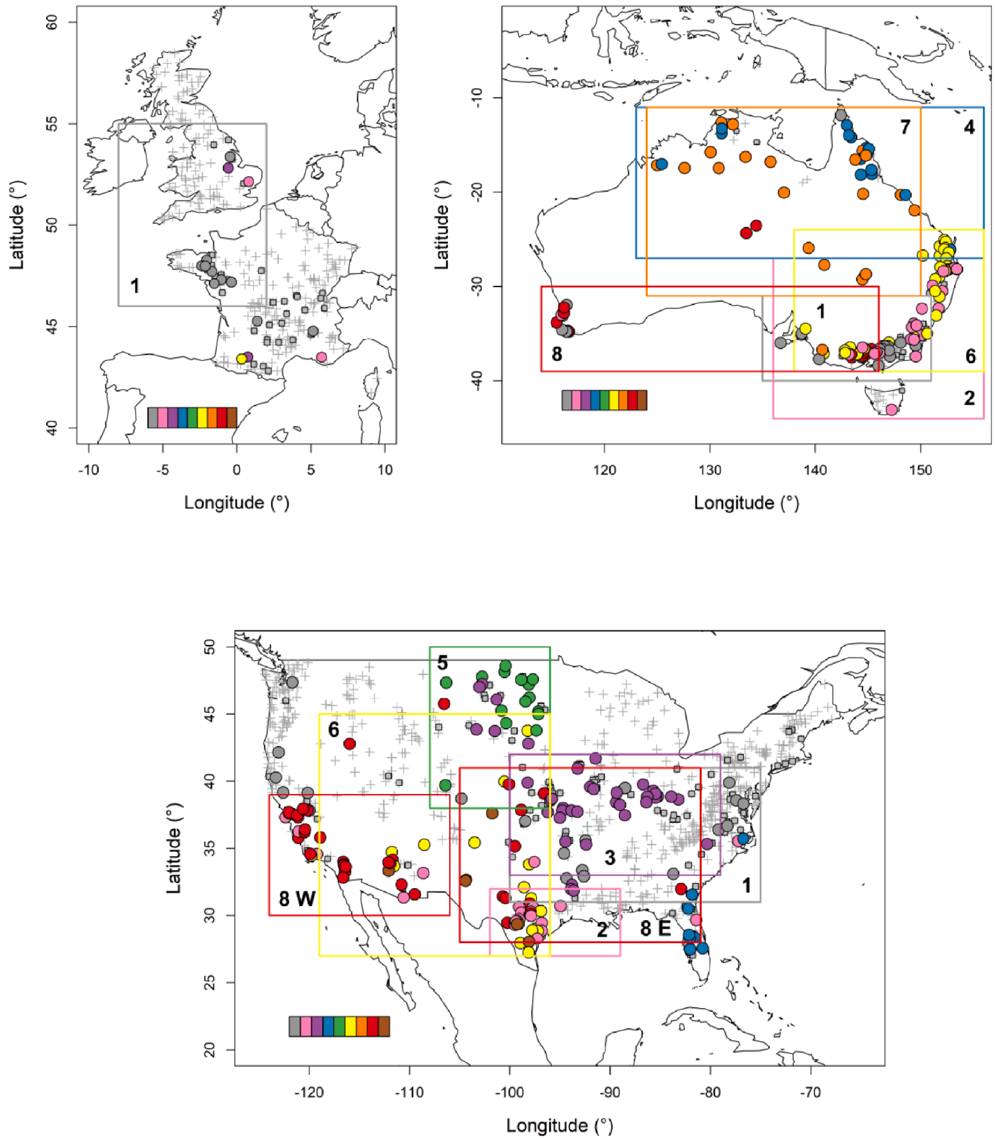

Fig. 8. Location of IRs in Australia, France, UK and the US, by Group (1–9; as indicated by color of the circles; color scheme follows that in Figs. 5 and 6).

observed along the coast in southern Australia. At the opposite extreme, the summer highly and extremely intermittent streams (Classes 10 and 12) of Kennard et al. (2010) and IRs from our Groups 4 and 7 are found in northern Australia. These links are substantial since the studies share a large proportion of gauging stations and correlated hydrological metrics.

The global classification developed here can be considered an extension of preexisting classifications encompassing additional temporal patterns that are missing in regional classifications (e.g., Group 5 and Group 7 are only found in the conterminous US and in Australia, respectively). Regardless of the large number of suitable gauging stations examined across the four countries, IRES experiencing freezing conditions are underrepresented in our classification. Examples in Antarctica, Switzerland and Norway can be found in the literature (Chinn and Mason, 2016; Robinson et al., 2016; Sauquet et al., 2020b). In addition, atypical local geological conditions may result in an unexpected hydrograph and require a novel group to be defined. This encourages us to extend data collection across other climates and other hydrogeological contexts. Despite the limitation of low coverage of data in areas experiencing continental, polar and alpine climates, the results presented here represent a major first attempt to classify and compare river flow regimes at a global scale.

4.4. Long-term trend analysis in no-flow conditions

Several analyses have been conducted to study the impact of long-term climate variability on low flows, in Australia (Chiew and McMahon, 1993; Zhang et al., 2016), in France (Renard et al., 2008; Giuntoli et al., 2013), in the UK (Hannaford and Buys, 2012; Hannaford, 2015) and in the US (e.g., Douglas et al., 2000; Small et al., 2006; Kam and Sheffield, 2016; Ahn and Palmer, 2015). The present study is, to our knowledge, the first to focus on flow intermittence at the global scale. Our findings are, for the most part, in agreement with those from the previous cited works.

In Australia, the 1982–1983 drought affected the east part of the country (Gibbs, 1984). Very low precipitation over the period of April 1982-February 1983 was recorded in southeastern Australia. Prevailing, extremely dry conditions were responsible for huge dust storms and one of the most deadly bushfires in the history of Australia in February 1983 (known as the 1983 “Ash Wednesday bushfires”, e.g. Blanchi et al., 2014). From the mid-1990s to 2009, southeastern Australia experienced a prolonged sequence of yearly precipitation deficit known as the “Millennium Drought” (Leblanc et al., 2012; van Dijk et al., 2013), peaking in 2006 with the lowest average rainfall for South Australia since 1900. A high proportion of no-flow conditions were observed in

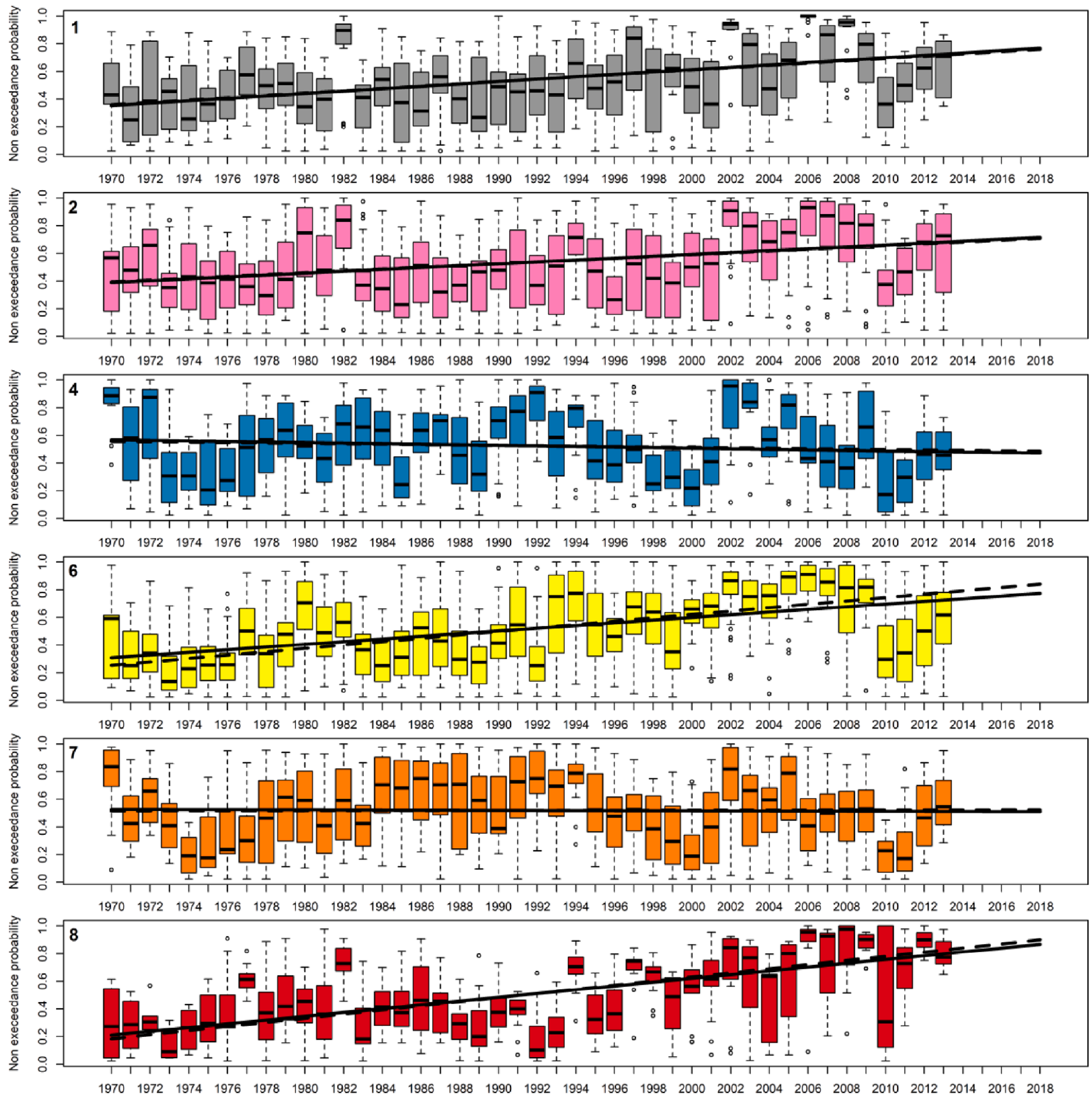

Fig. 9. Box plot of the empirical non exceedance probability of annual *F*0 for Australia, per Group. Years are labelled on the x-axis using the start of each water year.

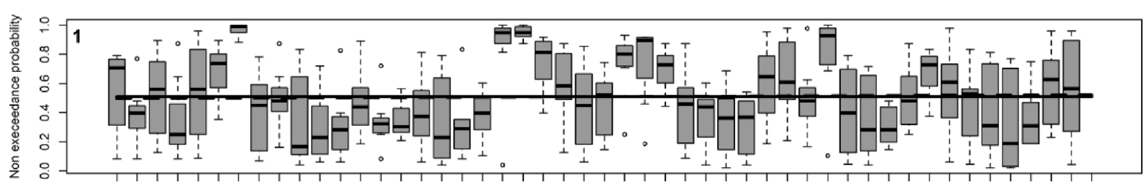

Fig. 10. Box plot of the empirical non exceedance probability of annual *F*0 for France and the UK, per Group. Years are labelled on the x-axis using the start of each water year.

rivers within Groups 1, 2, 6 and 8 for the corresponding period (Fig. 9). The decreasing trend found in *Q*90 in southern Australia (temperate climate zone) is in accordance with results obtained for Groups 1, 2, 6 and 8. No change was found for Groups 4 and 7 with geographical domains partly overlapping central Australia where no significant trends in *Q*90 were detected. This is in agreement with Zhang et al. (2016), who found temporal changes in hydrology varied with latitude.

The impact of several major drought events in Europe during the period 1970–2013 (Spinoni *et al.*, 2015; Hanel et al., 2018) was also apparent (Fig. 10), with above normal no-flow frequencies observed during the droughts. Deficits in precipitations from December 1975 until August 1976 were particularly high in southern UK and northern France, comparative to the Mediterranean region (Vidal *et al.*, 2010; Zaidman et al., 2002), causing a high proportion of no-flow events in Group 1 (Fig. 10). Note that flow intermittence in 2003 and in 2015 was close to average conditions, with a median non-exceedance probability dispersed around 50%. The 2003 European heat-wave event (García--Herrera et al., 2010) produced an agricultural drought, with more impact on soil moisture than on river flow (Vidal *et al.*, 2010). The 2015 European drought event (Laaha et al., 2017) mainly affected central

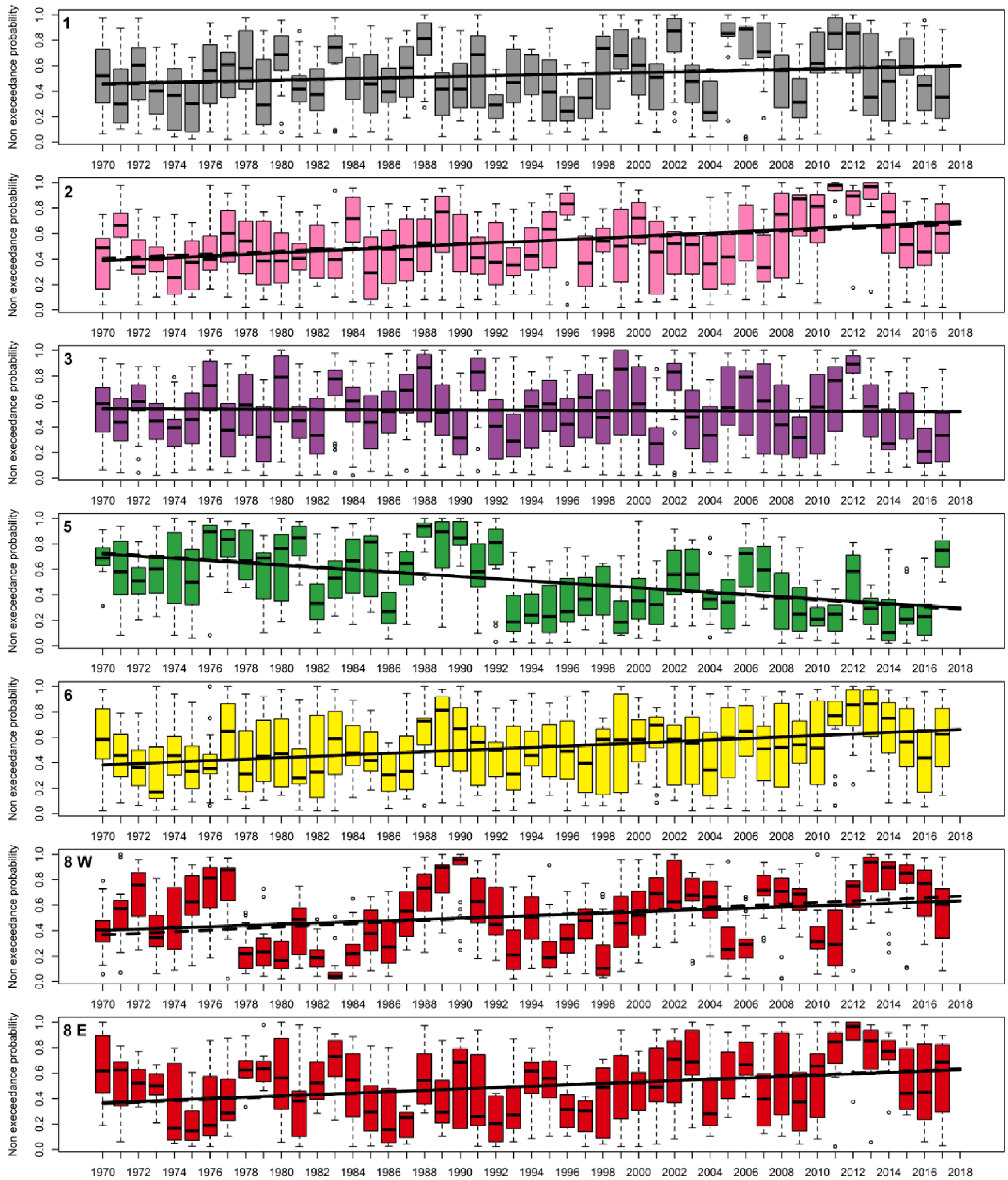

Fig. 11. Box plot of the empirical non exceedance probability of annual *F*0 for the US, per Group. Years are labelled on the x-axis using the start of each water year.

Europe, spanning from eastern France to southern Poland and northern Romania, however there was no evidence of general change in low flows for the UK, nor for France. Giuntoli et al. (2013) showed evidence of downward trends in annual minimum discharge in southern France while no change was detected in northern France; no IRs which met our selection criteria are gauged in areas where these changes were detected. We also found no significant trend in flow intermittence for Group 1 with all IRs located in northern France and in the UK.

In the US, the year 1988 stands out and corresponds to the "North American Drought of 1988" (Namias, 1991; Fig. 11). This was one of the most severe and extensive droughts of recent times in the US, affecting the Northern Plains in particular. Starting in 1987 and continuing until 1992, this multi-year event was accompanied by two heat waves in summer 1988. A significant multi-year drought occurred in California during the period 2007–2009 (California Department of Water Resources, 2010) and its effect on river flows is noticeable for Group 8 with above average flow intermittence conditions.

There are many other intermittency indices, some of which also display trends in European rivers (Tramblay et al., 2020) and may also be important on other continents. However, *F*0 is the most widely used metric for characterization; therefore, this study chose *F*0 as a starting point and suggests additional metrics be examined in further studies.

5. Conclusions

Here we characterized and classified the flow regimes of non-perennial rivers using data sourced from a large collection of gauging stations monitoring unregulated rivers in four countries and representing a range of climate conditions. Priority was given to near-natural flow regimes in gauging station selection over proportionate representation

Table 5
Statistic tests used for trend analysis. Significant changes are in bold characters.

	Group	Flow intermittence Corrected p-value	Tau	Theil-Sen Slope	Aridity Corrected p-value	Tau	Theil-Sen Slope	Winter temperature Corrected p-value	Tau	Theil-Sen Slope
Australia	**1**	**<0.001**	**0.410**	**0.833**	**0.026**	**−0.209**	**−0.005**	**0.002**	**0.303**	**0.015**
	2	**0.030**	**0.297**	**0.656**	**0.030**	**−0.175**	**−0.004**	**0.000**	**0.322**	**0.017**
	4	0.108	−0.076	−0.145	0.178	−0.102	−0.002	0.140	0.141	0.012
	6	**0.001**	**0.424**	**1.225**	**0.024**	**−0.189**	**−0.003**	**0.001**	**0.301**	**0.017**
	7	0.994	−0.002	0.015	0.793	−0.019	0.000	0.176	0.123	0.011
	8	**<0.001**	**0.516**	**1.492**	**0.007**	**−0.235**	**−0.003**	**0.002**	**0.241**	**0.012**
France and UK	1	0.836	0.018	0.050	0.566	−0.056	−0.001	0.144	0.145	0.018
Conterminous US	**1**	**0.049**	**0.129**	**0.304**	0.794	−0.019	0.000	0.075	0.166	0.029
	2	**0.002**	**0.314**	**0.559**	0.333	−0.094	−0.002	**0.026**	**0.225**	**0.030**
	3	0.742	−0.039	−0.037	0.282	0.080	0.002	0.066	0.176	0.035
	5	**0.001**	**−3.361**	**−0.926**	**0.031**	**0.183**	**0.003**	0.088	0.165	0.050
	6	**< 0.001**	**4.971**	**0.579**	0.451	−0.048	−0.001	**0.006**	**0.218**	**0.032**
	8 W	0.125	1.533	0.637	0.345	−0.073	−0.001	**0.026**	**0.214**	**0.026**
	8 E	0.066	1.841	0.568	0.519	−0.043	−0.001	**0.015**	**0.215**	**0.033**

of intermittence or types of intermittent river across the contributing countries. From the 1356 selected stations, 308 had a mean annual frequency of no flows ≥5 days/year and were assigned as "intermittent". The classification included different aspects of flow intermittence, and will be useful to assess the impact of no-flow periods on biological communities and ecosystem processes. Our findings also suggest that the proportion of IRES varies in space. Under a temperate climate, this proportion is certainly underestimated due to the priority given to gauging rivers in medium to large basins and in urban areas where water resources are sufficient enough to develop human activities and where the human population needs to be protected against extreme events.

A simple aridity index was found to be the most relevant factor discriminating intermittent from perennial rivers at the global scale. The link between aridity and flow intermittence identified here may provide a first insight into the risk of individual rivers becoming intermittent due to change in climate. For example, a modified *AI* could be computed for different scenarios of shifts in mean annual rainfall and temperature. The considered river could be categorized thereafter according to the UNEP classification ("arid & semi-arid", "dry sub-humid", "humid") and its probability of being intermittent under the modified climate given by the proportion of IRs within the aridity class provided by Table 3.

The classification also defined a basis for trend detection in annual frequency of no flows at a regional scale, with conclusions supporting those obtained for low flows of near natural basins in the countries examined. At the global scale, the global warming observed in recent years may not necessarily have led to more flow intermittence, but such a conclusion must be viewed with caution and requires further investigation as it is based on a finite set of gauged stations, data and analyses.

Information on how flow intermittence develops in both time and space is still sparse, partly due to the lack of gauged or otherwise monitored IRES. In the absence of information on IRES location, options to identify them include conducting field surveys along river networks (e.g., Turner and Richter, 2011; Assendelft and van Meerveld, 2019; Sefton *et al.*, 2019), utilising aerial images (e.g., Spence and Mengistu, 2016; González-Ferreras and Barquín, 2017) and supporting citizen science projects powered by smartphone apps (e.g., https://crowdwater.ch/en/welcome-to-crowdwater/). However, technical developments and analyses are still required to evaluate the benefit of these methods, to convert the information they provide into useful hydrological metrics and to combine this new information with records obtained and hydrological metrics derived from the more conventional observation network.

CRediT authorship contribution statement

Eric Sauquet: Conceptualization, Methodology, Validation, Software, Formal analysis, Resources, Supervision, Writing - original draft, Writing - review & editing. **Margaret Shanafield:** Validation, Resources, Writing - original draft, Writing - review & editing. **John C. Hammond:** Validation, Formal analysis, Software, Resources, Writing - original draft, Writing - review & editing. **Catherine Sefton:** Validation, Resources, Writing - original draft, Writing - review & editing. **Catherine Leigh:** Validation, Conceptualization, Writing - original draft, Writing - review & editing. **T. Datry:** Writing - original draft, Conceptualization, Project administration, Funding acquisition.

Declaration of Competing Interest

The authors declare that they have no known competing financial interests or personal relationships that could have appeared to influence the work reported in this paper.

Acknowledgement

This work is one aspect of the international research project "Intermittent River Biodiversity Analysis and Synthesis" (IRBAS, irbas.inrae.fr). We thank the editor and two anonymous reviewers for their helpful critique, which improved this manuscript.

Appendix A. – Calculation of hydrological metrics

The characteristics of flow intermittence. The frequency of no-flow conditions $F0$ is the percentage of the time with $Q \leq 1$ l/s. The pth quantile Qp is the daily discharge value exceeded p% of time. Metrics related to no-flow events are computed. A no-flow event starts when $Q \leq 1$ l/s and will last until $Q > 1$ l/s. The metrics *meanD*, *medianD*, and *sD* are the mean, median and standard deviation of the duration of no-flow events, respectively. The no-flow events have been identified for each water year to estimate *meanN*, *medianN*, and *sdN,* which are the mean, median and standard deviation of the number of no-flow events per year, respectively.

The maximal duration of the continuous sequence of no flow within the year, exceeded on average every five years ($D80$). Maximum duration of consecutive no flows (D) are sampled by block maxima approach and $D80$ is defined as the empirical 80th percentile of cumulative distribution function of D.

The mean and dispersion of the occurrence of no flows within the year (θ and *r*). These two variables are circular statistics. Each day *i* with no flow is converted into an angular (t_i) and represented by a unit vector with rectangular coordinates (cos(t_i); sin(t_i)). The mean of the cosines and sines defines a representative vector. The value for θ is obtained by calculating the inverse tangent of the angle of the mean vector and the norm of the mean vector provides a measure of the regularity in the dates (a value close to one indicates a high concentration around θ while a value close to zero indicates no seasonality). To account for the shift in the timing of winter in the two hemispheres (December to February in the Northern Hemisphere; June to August in the Southern Hemisphere), the constant -π or π is added to θ for Australian gauged basins when θ occurred between 1st July and 31st December or 1st January and 30th June, respectively.

Seasonal predictability of no-flow events (*Sd*6). This metric was formerly introduced by Gallart et al. (2012) and uses monthly discharge:

$$Sd6 = 1 - meanF06wm/meanF06dm$$

where *meanF*06*dm* and *meanF*06*wm* represent the average frequency of month with no-flow for the contiguous six driest months of the year and for the remaining six wetter months, respectively. The *Sd*6 descriptor is computed here using monthly frequencies of days with no flow.

The seasonal recession time scale (*Drec*). This duration based on the hydrograph defined by the 30-day moving average of the 365 long term mean daily discharges Q_{d} –, $d = 1,\ldots,365$. The day with the maximal value within the 365 values is the start of the water year. *Drec* is defined by the portion between the median and the 90th quantile of Q_{d} – of the falling limb.

The concavity index (*Ic*). This descriptor is a dimensionless measure of the contrast between low-flow and high-flow regimes derived from quantiles of the Flow Duration Curve:

$$IC = \frac{Q_{10} - Q_{99}}{Q_{1} - Q_{99}}$$

The base flow index (*BFI*). The method used to compute *BFI* is the algorithm suggested by the Institute of Hydrology (1980). Baseflow volume is obtained by hydrograph separation applying a smoothed minima approach to the discharge time series divided into 5-day non-overlapping blocks. The base flow index *BFI* is the ratio of baseflow to total flow.

The median duration of runoff events (*medianDr*). Daily values for runoff are obtained by subtracting the base flow from the observed river flow. The most severe runoff events within each year are selected. The spread of the upper part of the hydrographs is related to the quick subsurface runoff component. For each of the hydrographs $Q(t)$, the peak value *Qmax* and thereafter the duration for which $Q(t) > Qmax/2$ are calculated. Finally, *medianDr* is the median of the durations.

Appendix B. – Description of the groups obtained by cluster analysis

Group 1 is, in the dataset, the flow intermittence regime observed under humid subtropical climate and temperate oceanic climate in the three continents. Characteristics are typical of rainfall-fed regimes of intermittent rivers ($F0 < 10\%$ and $medianN = 0$ for most of the basins). Low flows and probably flow intermittence are likely due to evapotranspiration processes in summer. No-flow events are short (*medianD* around 10 days) and highly seasonal (46 out of the 51 IRs display *r* above 0.7), occurring in late summer (March or April in Australia, August or September in Europe and in the US).

Group 2 IRs are mainly located in the eastern US and southeastern Australia. Group 2 is similar to Group 1 in terms of duration and frequency of no-flow events and is the group ranked 2nd in terms of size (67 IRs). The two groups differ in both the timing and predictability of no-flow events (earlier in summer with a less pronounced seasonality than Group 1). IRs from Group 2 tend to be more intermittent (the median of *F*0 is 15 d/yr) and flashier (in terms of *Q*01 and *medianDr*) than IRs from Group 1.

Group 3 is also similar to Groups 1 and 2 in terms of duration and frequency of no-flow events. Basins from Group 3 experience more no flows than the two previous Groups (*F*0 around 22 d/yr). They are found in the central US and Europe. No flows occur usually around September for the US. The dispersion of the occurrence of no-flow days within the year (median $r \sim 0.73$) is between Group 1 (median $r \sim 0.85$) and Group 2 (median $r \sim 0.63$). No-flow events are more frequently observed ($medianN > 0$ for almost 50% of the basins) than in Groups 1 and 2.

Group 4 IRs are similar to those in Groups 1–3 in terms of flow permanence *F*0 (median around 10%). They differ by their location (they are found in areas experiencing equatorial, subtropical or tropical climate in northwestern Australia and in Florida) and their seasonality (no-flow events are observed in spring). Intermittence is not observed every year. *Q*90 within this group can be above 1 l/s.

Group 5 are found exclusively within northcentral US, in regions with winter temperatures below zero, indicating the flow regimes of this group are likely to be partly influenced by snow processes. The median date of occurrence of no-flow events is observed in autumn or winter, but the seasonality of flow intermittence is not well pronounced. Small values for *r* are due to continental climate leading to two no-flow periods, one induced by freezing in winter and the other by evapotranspiration processes in summer.

Group 6 pools moderate and harsh IRs, all but one from southern Australia and western US. *F*0 ranges between 6% and 86% with a median value of 26%. Group 6 comprises IRs with the highest values of *medianN* ($\sim$ 2.5 no-flow events per year): no flows tend to be divided into several events and these events are distributed within the year, leading to low values for *r* and no strong seasonal pattern. Only 10 among the 50 basins have $Q90 > 0$.

Characteristics of Group 7 are typical of harsh IRs located in central Australia. No-flow events are observed in late winter and early spring. All basins display $Q90 = 0$, $medianN > 0$, and climates for 6 of the 20 basins are dry sub-humid to arid.

Group 8 and Group 7 IRs are very similar in terms of flow intermittence (medians of *F*0 close to 40%, for the two groups). Those of Group 8 differ mainly in the way the no flows are distributed within the year (late summer for Group 8 and spring for Group 7). Several no-flow events can be expected within the year (medians of $medianN = 2$ for both groups) and a median no-flow event for Group 8 IRs persists 25 days (median of *medianD*), which is shorter than a median no-flow event for Group 7 IRs (21 days).

Group 9 IRs are ephemeral streams with few days of flow (on average >3 d/yr with $F0 \sim 98\%$). They are found in the south central US under arid and semi-arid conditions. They experience flashy runoff events ($medianDr = 1$ d). The seasonality of flow intermittence is not pronounced and values for *r* are close to 0 due to extended periods of little to no rainfall.

References

Abatzoglou, J., Dobrowski, S.Z., Parks, S.A., Hegewisch, K.C., 2018. TerraClimate, a high-resolution global dataset of monthly climate and climatic water balance from 1958–2015. Sci. Data 5, 170191. https://doi.org/10.1038/sdata.2017.191.

Ahn, K., Palmer, R., 2015. Trend and variability in observed hydrological extremes in the United States. J. Hydrol. Eng. https://doi.org/10.1061/(ASCE)HE.1943-5584.0001286, 04015061.

Archfield, S.A., Kennen, J.G., Carlisle, D.M., Wolock, D.M., 2014. An objective and parsimonious approach for classifying natural flow regimes at a continental scale. River Res. Appl. 30 (9), 1166–1183.

Assendelft, R.S., (Ilja) van Meerveld, R.S., 2019. A low-cost, multi-sensor system to monitor temporary stream dynamics in mountainous headwater catchments. Sensors 19 (21), 4645. https://doi.org/10.3390/s19214645.

Assunção, R.M., Neves, M.C., Câmara, G., Freitas, C.D.C., 2006. Efficient regionalization techniques for socio-economic geographical units using minimum spanning trees. Int. J. Geogr. Inf. Sc. 20, 797–811.

Barker, L., Hannaford, J., Parry, S., Smith, K.A., Tanguy, M., Prudhomme, C., 2019. Historic hydrological droughts 1891–2015: systematic characterisation for a diverse set of catchments across the UK. Hydrol. Earth Syst. Sci. 23, 4583–4602. https://doi.org/10.5194/hess-23-4583-2019.

Baston, D., 2020. exactextractr: Fast Extraction from Raster Datasets using Polygons. https://isciences.gitlab.io/exactextractr/.

Beaufort, A., Carreau, J., Sauquet, E., 2019. A classification approach to reconstruct local daily drying dynamics at headwater streams. Hydrol. Process. 33, 1896–1912.

Beaufort, A., Lamouroux, N., Pella, H., Datry, T., Sauquet, E., 2018. Extrapolating regional probability of drying of headwater streams using discrete observations and gauging networks. Hydrol. Earth Syst. Sci. 22, 3033–3051.

Blanchi, R., Leonard, J., Haynes, K., Opie, K., James, M., Dimer de Oliveira, F., 2014. Environmental circumstances surrounding bushfire fatalities in Australia 1901–2011. Environ. Sci. Policy 37, 192–203.

Bond, N., McMaster, D., Reich, P., Thomson, J.R., Lake, P.S., 2010. Modelling the impacts of flow regulation on fish distributions in naturally intermittent lowland streams: an approach for predicting restoration responses. Freshwater Biol. 55, 1997–2010. https://doi.org/10.1111/j.1365-2427.2010.02421.x.

Burn, D.H., 1997. Catchment similarity for regional flood frequency analysis using seasonality measures. J. Hydrol. 202, 212–230. https://doi.org/10.1016/S0022-1694(97)00068-1.

California Department of Water Resources, 2010. California's Drought of 2007–2009: An Overview. September 2010, 116 pp.

Buttle, J.M., Boon, S., Peters, D.L., Spence, C., (Ilja) van Meerveld, H.J., Whitfield, P.H., 2012. An overview of temporary stream hydrology in Canada. Can. Water Resour. J./Revue Canadienne Des Ressources Hydriques 37 (4), 279–310. https://doi.org/10.4296/cwrj2011-903.

Castellarin, A., Burn, D.H., Brath, A., 2001. Assessing the effectiveness of hydrological similarity measures for flood frequency analysis. J. Hydrol. 241, 270–285. https://doi.org/10.1016/S0022-1694(00)00383-8.

Catalogne, C., 2012. Amélioration des méthodes de prédétermination des débits de référence d'étiage en sites peu ou pas jaugés (Ph.D. dissertation) (in French). Univ. Grenoble.

Cherlet, M., Hutchinson, C., Reynolds, J., Hill, J., Sommer, S., von Maltitz, G. (Eds.), 2018. World Atlas of Desertification. Publication Office of the European Union, Luxembourg.

Chiew, F.H.S., McMahon, T.A., 1993. Detection of trend or change in annual flow of Australian rivers. Int. J. Climatol. 13, 643–653.

Chinn, T., Mason, P., 2016. The first 25 years of the hydrology of the Onyx River, Wright Valley, Dry Valleys Antarctica. Polar Record 52 (262), 16–65. https://doi.org/10.1017/S0032247415000212.

Couturier, B., Fourneaux, J.C., 1998. Les relations karst-rivière dans les calcaires barrémo-bédouliens du Diois (Drôme – France). Exemple de la Gervanne. Bull. Eng. Geol. Environ. 57 (2), 207–212. https://doi.org/10.1007/s100640050037.

Datry, T., Larned, S.T., Tockner, K., 2014. Intermittent rivers: a challenge for freshwater ecology. Bioscience 64, 229–235.

D'Ambrosio, E., De Girolamo, A.M., Barca, E., Rulli, M.C., 2017. Characterising the hydrological regime of an ungauged temporary river system: a case study. Environ. Sci. Pollut. Res. 24, 13950–13966. https://doi.org/10.1007/s11356-016-7169-0.

De Girolamo, A.M., Bouraoui, F., Buffagni, A., Pappagallo, G., Lo Porto, A., 2017. Hydrology under climate change in a temporary river system: potential impact on water balance and flow regime. River Res. Appl. 33, 1219–1232. https://doi.org/10.1002/rra.3165.

Döll, P., Schmied, H.M., 2012. How is the impact of climate change on river flow regimes related to the impact on mean annual runoff? A global-scale analysis. Environ. Res. Lett. 7 (2012), 1–11. https://doi.org/10.1088/1748-9326/7/1/014037.

Douglas, E.M., Vogel, R.M., Kroll, C.N., 2000. Trends in flood and low flows in the United States: impact of spatial correlation. J. Hydrol. 1–2, 90–105.

Dudley, R.W., Hirsch, R.M., Archfield, S.A., Blum, A.G., Renard, B., 2020. Low streamflow trends at human-impacted and reference basins in the United States. J. Hydrol. 580, 124254.

Eng, K., Wolock, D.M., Dettinger, M.D., 2015. Sensitivity of intermittent streams to climate variations in the USA. River Res. Appl. 32 (5), 885–895. https://doi.org/10.1002/rra.2939.

Falcone, J.A., 2011. GAGES–II, Geospatial Attributes of Gages for Evaluating Streamflow [digital spatial dataset], available at <http://water.usgs.gov/GIS/metadata/usgswrd/XML/gagesII_Sept2011.xml>.

Falcone, J.A., Carlisle, D.M., Wolock, D.M., Meador, M.R., 2010. GAGES: A stream gage database for evaluating natural and altered flow conditions in the conterminous United States. Ecology 91 (2), 621.

Gallart, F., Prat, N., García-Roger, E.M., Latron, J., Rieradevall, M., Llorens, P., Barberá, G.G., Brito, D., De Girolamo, A.M., Lo Porto, A., Buffagni, A., Erba, S., Neves, R., Nikolaidis, N.P., Perrin, J.L., Querner, E.P., Quiñonero, J.M., Tournoud, M.G., Tzoraki, O., Skoulikidis, N., Gómez, R., Sánchez-Montoya, M.M., Froebrich, J., 2012. A novel approach to analysing the regimes of temporary streams in relation to their controls on the composition and structure of aquatic biota. Hydrol. Earth Syst. Sci. 16, 3165–3182. https://doi.org/10.5194/hess-16-3165-2012.

García-Herrera, R., Díaz, J., Trigo, R.M., Luterbacher, J., Fischer, E.M., 2010. A Review of the European summer heat wave of 2003. Crit. Rev. Env. Sci. Technol. 40 (4), 267–306. https://doi.org/10.1080/10643380802238137.

Gibbs, W.J., 1984. The great Australian drought: 1982–1983. Disasters 8 (2), 89–104.

Giuntoli, I., Renard, B., Vidal, J.-P., Bard, A., 2013. Low flows in France and their relationship to large-scale climate indices. J. Hydrol. 482, 105–118. https://doi.org/10.1016/j.jhydrol.2012.12.038.

Gnann, S., Woods, R., Howden, N., 2019. Is There a Baseflow Budyko Curve? Water Resour. Res. 55 (4), 2838–2855. https://doi.org/10.1029/2018WR024464.

González-Ferreras, A.M., Barquín, J., 2017. Mapping the temporary and perennial character of whole river networks. Water Resour. Res. 53 (8), 6709–6724.

Guo, D., 2008. Regionalization with dynamically constrained agglomerative clustering and partitioning (REDCAP). International Journal of Geographical Information Science 22, 801–823.

Halaburka, B.J., Lawrence, J.E., Bischel, H.N., Hsiao, J., Plumlee, M.H., Resh, V.H., Luthy, R.G., 2013. Economic and ecological costs and benefits of streamflow augmentation using recycled water in a California coastal stream. Environ. Sci. Technol. 47 (19), 10735–10743. https://doi.org/10.1021/es305011z.

Hammond, J.C., Saavedra, F.A., Kampf, S.K., 2018. How does snow persistence relate to annual streamflow in mountain watersheds of the Western US with wet maritime and dry continental climates? Water Resour. Res. 54 (4), 2605–2623.

Hanel, M., Rakovec, O., Markonis, Y., Máca, P., Samaniego, L., Kyselý, J., Kumar, R., 2018. Revisiting the recent European droughts from a long-term perspective. Sci. Rep. 8, 9499. https://doi.org/10.1038/s41598-018-27464-4.

Hannaford, J., Buys, G., 2012. Trends in seasonal river flow regimes in the UK. J. Hydrol. 475, 158–174. https://doi.org/10.1016/j.jhydrol.2012.09.044.

Hannaford, J., 2015. Climate-driven changes in UK river flows: a review of the evidence. Prog. Phys. Geogr. 39 (1), 29–48. https://doi.org/10.1177/0309133314536755.

Harrigan, S., Hannaford, J., Muchan, K., Marsh, T., 2018a. Designation and trend analysis of the updated UK Benchmark Network of river flow stations: the UKBN2 dataset. Hydrol. Res. 49 (2), 552–567. https://doi.org/10.2166/nh.2017.058.

Harrigan, S., Prudhomme, C., Parry, S., Smith, K., Tanguy, M., 2018b. Benchmarking ensemble streamflow prediction skill in the UK. Hydrol. Earth Syst. Sci. 22, 2023–2039. https://doi.org/10.5194/hess-22-2023-2018.

Helsel, D.R., Frans, L.M., 2006. Regional Kendall test for trend. Environ. Sci. Technol. 40 (13), 4066–4073.

Hodgkins, G.A., Whitfield, P.H., Burn, D.H., Hannaford, J., Renard, B., Stahl, K., Fleig, A. K., Madsen, H., Mediero, L., Korhonen, J., Murphy, C., Wilson, D., 2017. Climate-driven variability in the occurrence of major floods across North America and Europe. J. Hydrol. 552, 704–717. https://doi.org/10.1016/j.jhydrol.2017.07.027.

Huxter, E.H.H., (Ilja) van Meerveld, H.J., 2012. Intermittent and Perennial Streamflow Regime Characteristics in the Okanagan. Can. Water Resour. J./Revue canadienne des ressources hydriques 37 (4), 391–414. https://doi.org/10.4296/cwrj2012-910.

Jaeger, K.L., Olden, J.D., Pelland, N.D., 2014. Climate change poised to threaten hydrologic connectivity and endemic fishes in dryland streams. Proc. Natl. Acad. Sci. U.S.A. https://doi.org/10.1073/pnas.1320890111.

Jeannin, P.-Y., Hessenauer, M., Malard, A., Chapuis, V., 2016. Impact of global change on karst groundwater mineralization in the Jura Mountains. Sci. Total Environ. 541, 1208–1221. https://doi.org/10.1016/j.scitotenv.2015.10.008.

Kam, J., Sheffield, J., 2016. Changes in the low flow regime over the eastern United States (1962–2011): variability, trends, and attributions. Clim. Change 135 (3), 639–653.

Kennard, M.J., Pusey, B.J., Olden, J.D., Mackay, S.J., Stein, J.L., Marsh, N., 2010. Classification of natural flow regimes in Australia to support environmental flow management. Freshw. Biol. 55, 171–193. https://doi.org/10.1111/j.1365-2427.2009.02307.x.

Laaha, G., Gauster, T., Tallaksen, L.M., Vidal, J.-P., Stahl, K., Prudhomme, C., Heudorfer, B., Vlnas, R., Ionita, M., Van Lanen, H.A.J., Adler, M.-J., Caillouet, L., Delus, C., Fendekova, M., Gailliez, S., Hannaford, J., Kingston, D., Van Loon, A.F., Mediero, L., Osuch, M., Romanowicz, R., Sauquet, E., Stagge, J.H., Wong, W.K., 2017. The European 2015 drought from a hydrological perspective. Hydrol. Earth Syst. Sci. 21, 3001–3024. https://doi.org/10.5194/hess-21-3001-2017.

Larned, S.T., Datry, T., Arscott, D.B., Tockner, K., 2010. Emerging concepts in temporaryriver ecology. Freshwater Biol. 717–738. https://doi.org/10.1111/j.1365-2427.2009.02322.x.

Leblanc, M.J., Tweed, S.O., Van Dijk, A.I.J.M., Timbal, B., 2012. A review of historic and future hydrological changes in the Murray-Darling Basin. Global Planet. Change 80–81, 226–246.

Leigh, C., Boulton, A.J., Courtwright, J.L., Fritz, K., May, C.L., Walker, R.H., Datry, T., 2016. Ecological research and management of intermittent rivers: an historical review and future directions. Freshw. Biol. 61, 1181–1199.

Leigh, C., Datry, T., 2016. Drying as a primary hydrological determinant of biodiversity in river systems: a broad-scale analysis. Ecography. https://doi.org/10.1111/ecog.02230.

Leigh, C., Sheldon, F., 2008. Hydrological changes and ecological impacts associated with water resource development in large floodplain rivers in the Australian tropics. River Res. Appl. 24, 1251–1270. https://doi.org/10.1002/rra.1125.

Middleton, N., Thomas, D., (Eds.), 1997. World Atlas of Desertification, 2nd Edition, UNEP, London: Edward Arnold, 182 pp.

Moliere, D.R., Lowry, J.B.C., Humphrey, C.L., 2009. Classifying the flow regime of data-limited streams in the wet-dry tropical region of Australia. J. Hydrol. 367, 1–13.

Nadeau, T.-L., Rains, M.C., 2007. Hydrological connectivity between headwater streams and downstream waters: how science can inform policy. JAWRA J. Am. Water Resour. Assoc. 43, 118–133. https://doi.org/10.1111/j.1752-1688.2007.00010.x.

Namias, J., 1991. Spring and summer 1988 drought over the contiguous United States — causes and prediction. J. Clim. 4, 54–65.

Olden, J.D., Poff, N.L., 2003. Redundancy and the choice of hydrologic indices for characterizing streamflow regimes. River Res. Applic. 19, 101–121. https://doi.org/10.1002/rra.700.

Olden, J.D., Kennard, M.J., Pusey, B.J., 2011. A framework for hydrologic classification with a review of methodologies and applications in ecohydrology. Ecohydrology 5 (4), 503–518. https://doi.org/10.1002/eco.251.

Oueslati, O., De Girolamo, A.M., Abouabdillah, A., Kjeldsen, T.R., Lo Porto, A., 2015. Classifying the flow regimes of Mediterranean streams using multivariate analysis. Hydrol. Process. 29, 4666–4682. https://doi.org/10.1002/hyp.10530.

Peel, M.C., Finlayson, B.L., McMahon, T.A., 2007. Updated world map of the Köppen-Geiger climate classification. Hydrol. Earth Syst. Sci. 11, 1633–1644. https://doi.org/10.5194/hess-11-1633-2007.

Perez-Saez, J., Mande, T., Larsen, J., Ceperley, N., Rinaldo, A., 2017. Classification and prediction of river network ephemerality and its relevance for waterborne disease epidemiology. Adv. Water Resour. 110, 263–278.

Poff, N., 1996. A hydrogeography of unregulated streams in the United States and an examination of scale-dependence in some hydrological descriptors. Freshw. Biol. 36, 71–79. https://doi.org/10.1046/j.1365-2427.1996.00073.x.

Poff, N.L., Ward, J.V., 1989. Implications of streamflow variability and predictability for lotic community structure: a regional analysis of streamflow patterns. Can. J. Fish. Aquat. Sci. 46, 1805–1818.

Pumo, D., Caracciolo, D., Viola, F., Noto, L.V., 2015. Climate change effects on the hydrological regime of small non-perennial river basins. Sci. Total Environ. 542 (Part A), 76–92. https://doi.org/10.1016/j.scitotenv.2015.10.109.

Renard, B., Lang, M., Bois, P., Dupeyrat, A., Mestre, O., Niel, H., Sauquet, E., Prudhomme, C., Parey, S., Paquet, E., Neppel, L., Gailhard, J., 2008. Regional methods for trend detections: assessing field significance and regional consistency. Water Resour. Res. 44 (8), W08419. https://doi.org/10.1029/2007wr006268.

Renard, B., Thyer, M., 2019. Revealing hidden climate indices from the occurrence of hydrologic extremes. Water Resour. Res. 55, 7662–7681. https://doi.org/10.1029/2019WR024951.

Reynolds, L.V., Shafroth, P.B., Poff, N.L., 2015. Modeled intermittency risk for small streams in the Upper Colorado River Basin under climate change. J. Hydrol. 523, 768–780. https://doi.org/10.1016/j.jhydrol.2015.02.025.

Ribes, A., Thao, S., Vautard, R., Dubuisson, B., Somot, S., Colin, J., Planton, S., Soubeyroux, J.M., 2019. Observed increase in extreme daily rainfall in the French Mediterranean. Clim. Dyn. 52, 1095–1114.

Richter, B.D., Baumgartner, J.V., Powell, J., Braun, D.P., 1996. A method for assessing hydrologic alteration within ecosystems. Conserv. Biol. 10, 1163–1174.

Robinson, C.T., Tonolla, D., Imhof, B., Vukelic, R., Uehlinger, U., 2016. Flow intermittency, physico-chemistry and function of headwater streams in an Alpine glacial catchment. Aquat. Sci. 78, 327–341. https://doi.org/10.1007/s00027-015-0434-3.

Sauquet, E., Beaufort, A., Sarremejane, R., Thirel, G., 2020a. Assessing flow intermittence in France under climate change. Hydrol. Sci. J. submitted.

Sauquet, E., Catalogne, C., 2011. Comparison of catchment grouping methods for flow duration curve estimation at ungauged sites in France. Hydrol. Earth Syst. Sci. 15, 2421–2435. https://doi.org/10.5194/hess-15-2421-2011.

Sauquet, E., van Meerveld, I., Gallart, F., Sefton, C., Parry, S., Gauster, T., Laaha, G., Alves, M.H., Arnaud, P., Banasik, K., Beaufort, A., Bezdan, A., Datry, T., De Girolamo, A.M., Dörflinger, G., Elçi A., Engeland, K., Estrany, J., Fialho, A., Fortesa, J., Hakoun, V., Karagiozova T., Kohnova, S., Kriauciuniene, J., Morais, M., Ninov, P., Osuch, M., Reis, E., Rutkowska, A., Stubbington, R., Tzoraki, O., Żelazny, M., 2020. A catalogue of European intermittent rivers and ephemeral streams. Technical report SMIRES COST Action CA15113, 100 pp. https://doi.org/10.5281/zenodo.3763419.

Sefton, C.E.M., Parry, S., England, J., Angell, G., 2019. Visualising and quantifying the variability of hydrological state in intermittent rivers. Fundamental and Applied Limnology/Archiv für Hydrobiologie 193, 21–38. https://doi.org/10.1127/fal/2019/1149.

Sen, P.K., 1968. Estimates of the regression coefficient based on Kendall's tau. J. Am. Stat. Assoc. 63, 1379–1389. https://doi.org/10.2307/2285891.

Smakhtin, V.Y., Toulouse, M., 1998. Relationships between low-flow characteristics of South African streams. Water SA 24, 107–112.

Smakhtin, V.U., 2001. Low flow hydrology: a review. J. Hydrol. 240 (2001), 147–186.

Small, D., Islam, S., Vogel, R.M., 2006. Trends in precipitation and streamflow in the eastern U.S.: Paradox or perception? Geophys. Res. Lett. 33, L03403. https://doi.org/10.1029/2005GL024995.

Smith, K.A., Barker, L.J., Tanguy, M., Parry, S., Harrigan, S., Legg, T.P., Prudhomme, C., Hannaford, J., 2019. A multi-objective ensemble approach to hydrological modelling in the UK: an application to historic drought reconstruction. Hydrol. Earth Syst. Sci. 23, 3247–3268. https://doi.org/10.5194/hess-23-3247-2019.

Snelder, T.H., Datry, T., Lamouroux, N., Larned, S.T., Sauquet, E., Pella, H., Catalogne, C., 2013. Regionalization of patterns of flow intermittence from gauging station records. Hydrol. Earth Syst. Sci. 17, 2685–2699. https://doi.org/10.5194/hess-17-2685-2013.

Spence, C., Mengistu, S., 2016. Deployment of an unmanned aerial system to assist in mapping an intermittent stream. Hydrol. Process. 30, 493–500. https://doi.org/10.1002/hyp.10597.

Spinoni, J., Naumann, G., Vogt, J.V., Barbosa, P., 2015. The biggest drought events in Europe from 1950 to 2012. J. Hydrol.: Regional Studies 3, 509–524. https://doi.org/10.1016/j.ejrh.2015.01.001.

Stubbington, R., England, J., Wood, P.J., Sefton, C.E.M., 2017. Temporary streams in temperate zones: recognizing, monitoring and restoring transitional aquatic-terrestrial ecosystems. WIREs Water 4, e1223. https://doi.org/10.1002/wat2.1223.

Stubbington, R., Greenwood, A.M., Wood, P.J., Armitage, P.D., Gunn, J., Robertson, A.L., 2009. The response of perennial and temporary headwater stream invertebrate communities to hydrological extremes. Hydrobiologia 630, 299–312. https://doi.org/10.1007/s10750-009-9823-8.

Theil, H., 1950. A rank-invariant method of linear and polynomial regression analysis. I, II, III. Nederl. Akad. Wetensch. Proc. 53: 386–392, 521–525, 1397–1412.

Tramblay, Y., Rutkowska, A., Sauquet, E., Sefton, C., Laaha, G., Osuch, M., Albuquerque, T., Alves, M.-H., Banasik, K., Beaufort, A., Brocca, L., Camici, S., Zoltan, C., Dakhlaoui, H., De Girolamo, A.-M., Dörflinger, G., Gallart, F., Gauster, T., Hanich, I., Kohnová, S., Mediero, L., Plamen, N., Parry, S., Quintana-Segui, P., Tzoraki, O., Datry, T., 2020. Trends in flow intermittence for European Rivers. Hydrol. Sci. J. (in press).

Turner, D.S., Richter, H.E., 2011. Wet/dry mapping: using citizen scientists to monitor the extent of perennial surface flow in dryland regions. Environ. Manage. 47 (3), 497–505.

van Dijk, A.I.J.M., Beck, H.E., Crosbie, R.S., de Jeu, R.A.M., Liu, Y.Y., Podger, G.M., Timbal, B., Viney, N.R., 2013. The Millennium Drought in southeast Australia (2001–2009): natural and human causes and implications for water resources, ecosystems, economy, and society. Water Resour. Res. 49 https://doi.org/10.1002/wrcr.20123.

Vidal, J.-P., Martin, E., Franchistéguy, L., Habets, F., Soubeyroux, J.-M., Blanchard, M., Baillon, M., 2010. Multilevel and multiscale drought reanalysis over France with the Safran-Isba-Modcou hydrometeorological suite. Hydrol. Earth Syst. Sci. 14, 459–478. https://doi.org/10.5194/hess-14-459-2010.

Warfe, D.M., Pettit, N.E., Davies, P.M., Pusey, B.J., Hamilton, S.K., Kennard, M.J., Townsend, S.A., Bayliss, P., Ward, D.P., Douglas, M.M., Burford, M.A., Finn, M., Bunn, S.E., Halliday, I.A., 2011. The 'wet–dry' in the wet–dry tropics drives river ecosystem structure and processes in northern Australia. Freshw. Biol. 56, 2169–2195. https://doi.org/10.1111/j.1365-2427.2011.02660.x.

Westwood, C.G., England, J., Dunbar, M.J., Holmes, N.T.H., Leeming, D.J., Hammond, D., 2017. An approach to setting ecological flow thresholds for southern English chalk streams. Water Environ. 31 (4), 528–536. https://doi.org/10.1111/wej.12275.

World Meteorological Organization, 1989. Calculation of monthly and annual 30-year standard normals. WCDP-No. 10, WMO-TD/No. 341. Washington, D.C., U.S.A.

Yamazaki, D., Ikeshima, D., Sosa, J., Bates, P.D., Allen, G.H., Pavelsky, T.M., 2019. MERIT Hydro: a high-resolution global hydrography map based on latest topography dataset. Water Resour. Res. 55 (6), 5053–5073.

Yue, S., Wang, C., 2004. The Mann-Kendall test modified by effective sample size to detect trend in serially correlated hydrological series. Water Resour. Manage. 18, 201–218.

Yue, S., Wang, C., 2002. Regional streamflow trend detection with consideration of both temporal and spatial correlation. Int. J. Climatol. 22, 933–946. https://doi.org/10.1002/joc.781.

Yu, S., Bond, N.R., Bunn, S.E., Xu, Z., Kennard, M.J., 2018. Quantifying spatial and temporal patterns of flow intermittency using spatially contiguous runoff data. J. Hydrol. 559, 861–872.

Zaidman, M.D., Rees, H.G., Young,, A.R., 2002. Spatio-temporal development of streamflow droughts in north-west Europe. Hydrol. Earth Syst. Sci. 6, 733–751. https://doi.org/10.5194/hess-6-733-2002.

Zhang, X.S., Amirthanathan, G.E., Bari, M.A., Laugesen, R.M., Shin, D., Kent, D.M., MacDonald, A.M., Turner, M.E., Tuteja, N.K., 2016. How streamflow has changed across Australia since the 1950s: evidence from the network of hydrologic reference stations. Hydrol. Earth Syst. Sci. 20, 3947–3965. https://doi.org/10.5194/hess-20-3947-2016.

Zimmer, M.A., Kaiser, K.E., Blaszczak, J.R., Zipper, S.C., Hammond, J.C., Fritz, K.M., Costigan, K.H., Hosen, J., Godsey, S.E., Allen, G.H., Kampf, S., Burrows, R.M., Krabbenhoft, C.A., Dodds, W., Hale, R., Olden, J.D., Shanafield, M., DelVecchia, A. G., Ward, A.S., Mims, M.C., Datry, T., Bogan, M.T., Boersma, K.S., Busch, M.H., Jones, C.N., Burgin, A.J., Allen, D.C., 2020. Zero or not? Causes and consequences of zero-flow stream gage readings. WIREs Water 2020, e1436. https://doi.org/10.1002/wat2.1436.